Modelling and Design of PEM Fuel Cell Electric Military Armoured Vehicles Using a New Real-World Operation Profile Model

by

Scott Ormsby

Bachelor of Engineering, Royal Military College of Canada, 2011

A Thesis Submitted in Partial Fulfillment of the Requirements for the Degree of

MASTER OF APPLIED SCIENCE

in the Department of Mechanical Engineering

University of Victoria

Supervisory Committee

Modelling and Design of PEM Fuel Cell Electric Military Armoured Vehicles Using a New Real-World Operation Profile Model

By

Scott Ormsby

Bachelor of Engineering, Royal Military College of Canada, 2011

Supervisory Committee

Supervisor

Dr. Zuomin Dong, Department of Mechanical Engineering

Departmental Member

Dr. Andrew Rowe, Department of Mechanical Engineering

Abstract

Supervisory Committee

Supervisor

Dr. Zuomin Dong, Department of Mechanical Engineering

Departmental Member

Dr. Andrew Rowe, Department of Mechanical Engineering

The activities of the Department of National Defence (DND) account for more than half of the Government of Canada's greenhouse gas emissions. This research examines a clean energy propulsion solution to DND's carbon footprint using a Proton Exchange Membrane fuel cell (PEMFC) battery hybrid powertrain for military armoured vehicles as a means of meeting Canada's Greening Defence initiatives. Real-world military vehicle operational data is used to create the operation profile for military vehicle powertrain design requirements. Following the model-based design (MBD) approach, the vehicle dynamics, fuel cell system and powertrain system models implemented in MATLAB/Simulink are used to predict the vehicle's performance, emissions, and operational costs. This research examines the feasibility of using a fuel cell-battery electric powertrain for a military armoured vehicle and produces a feasible design solution to meet the identified vehicle operation and performance requirements. The fuel cost and powertrain component performance degradations are modelled to predict the operation costs of the clean vehicle with the benefits of reduced emissions, noise and thermal profiles. The results of this research suggest there are viable, clean propulsion system and energy storage system (ESS) configurations that satisfy the requirements of the operational profile of military armoured vehicles. This research serves as a foundation for the use of clean military vehicle propulsion in Canada.

Table of Contents

List of Figures

List of Tables

Acknowledgments

I wish to acknowledge the supervision and support of my thesis supervisor, Dr. Zuomin Dong, for providing me with the tools needed to explore clean energy and transportation. Without them, I would not have appropriately investigated what I consider to be the future of vehicle fleets and sustainable clean energy.

Secondly, I wish to thank my best friend Anthony Truelove for being my academic sounding board and anchor point during my time in British Columbia. Without your second set of eyes, I may not have been held accountable for the high standards I seek to attain for myself.

I want to thank Major Jonathon Fudge, Sergeant Alex Urquhart, Master Corporal Matt McFall, and the combat engineers of 4 ESR for their collaboration in this work. Without your expert subject matter input, this work would not have been possible.

Last but most definitely not least, I want to acknowledge the love of my life, Dr. Annelise Miller, for being patient and supportive during the road to my degree. Without you, I would not be the man I am today.

Dedication

I dedicate this work to the Canadian Armed Forces, with the goal of establishing a baseline foundation of work that will help develop a future green fleet to meet our government's climate change targets and provide a better world of tomorrow.

Glossary of Acronyms and Abbreviations

1-D	One-Dimensional
4 ESR	4th Engineering Support Regiment
ADM (Mat)	Assistant Deputy Minister of Materiel
BEV	Battery Electric Vehicle
CAF	Canadian Armed Forces
CFB	Canadian Forces Base
CSS	Combat Service Support
DC	Direct Current
DND	Department of National Defence
ESS	Energy Storage System
FCEV	Fuel Cell Electric Vehicle
GM	General Motors
GHG	Greenhouse Gas
GPS	Global Positioning System
HESS	Hybrid Energy Storage System
HEV	Hybrid Electric Vehicle
HWFET	Highway Fuel Economy Test
IED	Improvised Explosive Device
ICEV	Internal Combustion Engine Vehicle
ISS	In-Service Support
LCMM	Life Cycle Material Manager
LHD	Load-Haul-Dump
MAE	Maximum Allowable Error
MBD	Model Based Design
OCV	Open Circuit Voltage
PEMFC	Proton Exchange Membrane Fuel Cell
PI	Proportional Integral
QGIS	Quantum Graphing Information System
RCEME	Royal Canadian Electrical Mechanical Engineers

RTA	Range Training Area
RUL	Remaining Useful Life
SOC	State of Charge
SME	Subject Matter Expert
TAPV	Tactical Armoured Patrol Vehicle
UDDS	Urban Dynamometer Driving Schedule
UNFCC	United Nations Framework Convention on Climate Change
USD	United States Dollar
UTM	Universal Transverse Mercator

Chapter 1. Introduction

1.1. General Background

The impacts of humanity's collective carbon footprint have had a measurable and adverse impact on the planet's climate; the recognition of this fact has resulted in treaties such as the Paris Agreement signed in 2016 by 196 parties under the United Nations Framework Convention on Climate Change (UNFCCC) in an effort to reduce human-produced carbon emissions and slow global warming [1]. The Canadian government, in its own effort to address the climate crisis, has incorporated 'green' initiatives into its various policy frameworks.

One such policy is Canada's Defence Policy, titled *Strong, Secure, Engaged*, which has a sub-section under the section of 'Modernizing the Business of Defence' titled 'Greening Defence.' It estimates that the activities of National Defence account for more than half of the Government of Canada's greenhouse gas emissions, and one potential solution is to examine alternative energy options and their potential use in military operations [2]. While efforts are being made to hybridize the civilian fleet of vehicles owned by the Department of National Defence under the same 'Greening Defence' initiative, the military vehicle fleets themselves remain dependent on diesel and gasoline internal combustion engine vehicles (ICEVs) to operate. No Canadian military vehicle fleets as of yet have 'green' powertrains for propulsion, such as battery electric vehicles (BEVs), hybrid electric vehicles (HEV), or fuel cell electric vehicles (FCEVs) as powertrain configurations. Among these options, FCEVs are an emerging technology, nascent to the commercial market but slowly gaining traction and popularity, projected to represent 17% of the commercial market by 2050 [3]. FCEVs have advantages over other types of vehicle powertrains: they have a longer operational range and shorter refuelling times than BEVs, they generate high torque at low speeds similar to BEV or HEVs, they are greenhouse gas emission-free from pump-to-wheel as opposed to HEVs or ICEVs that use gasoline or diesel, and their power generated as a fuel converter matches that of ICEVs. It is for these reasons that an FCEV powertrain for armoured vehicles is being considered in this thesis.

1.2. Research Motivation

Investigating the feasibility of a Fuel Cell Electric Vehicle (FCEV) powertrain using a Proton Exchange Membrane fuel cell (PEMFC) system for armoured vehicles is not just beneficial for

the environment, but it comes with tactical advantages as well. Because there is no combustion process in the PEMFC system, the FCEV has a more negligible noise and thermal profile than that of a conventional internal combustion engine (ICE) vehicle, which are very desirable traits for the military in a theatre of operation. Canada's last major theatre of operation was in Afghanistan, from October 2001 to March 2014, and from then onward, how operations are conducted in the Canadian Armed Forces has been reshaped. While conventional warfare remains a viable threat, unconventional warfare has grown as a threat over the last two decades. Conflicts involve non-uniformed actors, can be asymmetric in nature, and can be enacted across non-contiguous battlespaces. This increased unpredictability leads to increased danger to military members across a wide range of activities, from offensive action to reconnaissance patrols, to combat service support (CSS) convoys - all of which benefit from increased passive protection through reduced noise and thermal profiles.

1.3. Research Objective

This research will examine the feasibility of military vehicle electrification using a PEMFC and battery hybrid electric powertrain system. This research uses a Model Based Design (MBD) approach employed by the automotive industry: models of the operation profile, PEMFC system, battery energy storage system (ESS), vehicle dynamics, and the complete FCEV powertrain system of an armoured vehicle are built and then used in the systems analyses and to guide design optimization. The model, implemented in MathWorks' MATLAB/Simulink, is used to evaluate the vehicles' performance, energy efficiency, emissions and lifecycle costs. Under different use patterns, the battery performance degradation model is to be incorporated into the model to accurately assess the FCEV cost. The vehicle will be tested in a simulated military tactical setting, estimating off-road driving over undulating terrain at nighttime during blackout conditions (no use of vehicle headlights). This scenario intends to make use of the advantages of the passive protection of the reduced noise and thermal profiles offered by an FCEV.

As there is limited academic data available regarding military 'driving cycles', an 'operation profile' is used instead in the vehicle model. The operation profile contains the speed, distance, elevation and environmental parameters the vehicle is subjected to. The vehicle's speed is determined based on Canadian Armed Forces doctrine for nighttime road movement [4]. At the same time, the distance and elevation will be constructed from a predetermined path in collaboration with the Canadian Army, who would be the end-user of such a vehicle.

Post-processing of the model data will be used to compare performance against a benchmark vehicle type currently used by the Canadian Armed Forces (ICEV), and vehicle usage will be associated with a cost of fuel consumption and powertrain wear and tear from usage.

1.4. Thesis Organization

The thesis is organized as follows:

Chapter 2 presents the literature review of previous research related to the modelling of vehicle operation profile, fuel cell electric vehicle powertrain architecture, and costs due to fuel consumption and the performance degradation of crucial powertrain components.

Chapter 3 provides an overview of the methodology used to design and build the operation profile of the military vehicle, introduces the vehicle powertrain system model, and the method for calculating the cost of vehicle use, considering both fuel consumption and the performance degradation of powertrain components.

Chapter 4 gives the simulation results using the newly introduced MATLAB/Simulink models of the military FCEV under the typical operations captured by the new operation profile.

Chapter 5 interprets and analyzes the results from the vehicle operation test simulations under given assumptions and discusses sources of potential errors.

Chapter 6 summarizes the findings of this work and offers areas that future work can build upon.

Chapter 2. Literature Review

At the time of writing, a search for information has shown that no FCEV military vehicles are known to have been implemented into service by any country, thus reducing the amount of available data to review in this particular field of study. Articles indicate that General Motors (GM) is working with the United States military to develop FCEV vehicles, while Kia is working with the Korean government to develop FCEVs, both as part of a greater electric drive initiative [5][6]. While both companies plan to deliver new electric capabilities by 2023 and 2024, neither article indicated a firm timeframe for implementing the fuel cell aspect of the vehicles. The closest approximation of an FCEV system resembling an armoured vehicle is FCEV commercial dump trucks, whose models have been studied to generate an armoured vehicle model in this work. Similarities between commercial dump trucks and military armoured vehicles include large mass and dynamic power loads, both of which play an important part in defining the vehicle model's powertrain architecture and high-level controller logic. Vehicles with large mass require more significant torque to accelerate and more energy to complete a duty cycle. The dynamic power loads need a vehicle controller capable of efficiently handling those changes in power control, sometimes involving power splitting to enable different powertrain system configurations for various vehicle applications.

2.1. Vehicle Driving Cycle and Operation Profile

2.1.1 Standard Vehicle Driving Cycles

A driving cycle is a series of data points of vehicle speed versus time, which is derived from the statistical data of vehicle operations. Different standard driving cycles are introduced via city and highway driving, or a combination of both, by various authoritative organizations of different countries and regions [7]. These driving cycles are used as standard vehicle operation templates to gauge the performance, fuel efficiency and emissions of vehicles, normally passenger cars and light vehicles. In addition, dedicated driving cycles for commercial trucks have been introduced as well [7].

While almost all existing vehicle performance evaluation and design modelling tools use these statistical driving cycles to calculate the needed propulsion power, vehicle performance, fuel efficiency and emissions, these are not feasible in representing a military armoured vehicle. While urban warfare involves movement in built-up residential areas, military vehicles in these

circumstances do not adhere to stopping for traffic signals. Quite often, military vehicles end up driving off-road for either tactical reasons or for practical ones: for instance, in wartime, bridges can be strategic control points that can be blockaded or even blown up to deny mobility to an adversary. As such, expected driving cycles outlined in the Urban Dynamometer Driving Schedule (UDDS), or fuel economy standards under the Highway Fuel Economy Test (HWFET), are not necessarily relevant to conditions seen by military vehicles. Factors such as gradient profiles for terrain must be considered, and typical driving cycles do not consider factors such as elevation.

2.1.2 Operation Profile of Special Vehicles

The operation profile is a more generic representation of vehicle operations and is used to describe the operational needs of special vehicle types, such as the commercial vehicle with a heavy payload that is variant with time (load cycle), or mining vehicles that operate on unique routes with changing payload and mine elevations [8].

When it comes to the military, there are different types of vehicles that are used. When introducing an operation profile for a particular class of specialty vehicles, there are three common factors that need to be considered: vehicle input, terrain input, and the software applications that process this data into a usable format.

Vehicle Input

Vehicles are what provide the speed and distance aspects of the operation profile. Presently, the academic work involving military vehicles has relied on the creation of operation profiles through the use of data loggers: driving over defined paths in real-time, collecting an aggregation of data that is then turned into an operation profile. One such study in Korea used data loggers attached to vehicles to capture data over sixteen different routes, collecting information such as engine torque, fuel consumption, and acceleration of the vehicle to generate their operation profile (which was referred to in their study as a ‘mission profile’). Global positioning system (GPS) coordinates were used to measure the vehicle speed and geographical features of the area [9].

There are limited studies involving operation profiles for military vehicles, and like the Korean study, they have relied upon data loggers to capture data points. Furthermore, they have also relied on standard driving cycles that were developed for passenger cars and light trucks operating on flat public roads. This presents numerous challenges in modeling realistic operating conditions for heavy military vehicles. Additional vehicle operation information,

including the rough terrain during off-road operation and the variant amount of vehicle payloads, has not been considered to accurately predict the needed propulsion power. Second, the armoured military vehicle presents a different power use pattern with the need to operate communication gear and other military hardware, and the new PEM fuel cell system offers other power distribution possibilities; these unique needs and new FCEV cannot be recorded using the conventional data logger approach.

Therefore, the introduction of a new operation profile model for armoured military vehicles will have to have a degree of novelty, but model validation will be challenging to perform, as there is no other publicly available military data to compare it against.

Terrain Input

Given that military operation profiles are created off of the literal beaten path, the terrain has a significant impact on defining the vehicle operation profile model. There are many environmental factors that impact the operation profile, the most notable of which is the changing gradient profile of uneven terrain, which requires the vehicle's controller to vary torque output to maintain constant speeds at different gradients. However, driving off-road also involves different surfaces that come into contact with the wheels, such as dirt, gravel, and grass (both wet and dry), all of which impact the coefficient of kinetic friction on the wheels. An accident reconstruction group from [10] has provided data in Table 1 highlighting the different coefficients of friction based on surface type.

Table 1: Kinetic coefficients of friction based on the surface type [10]

Description of Road Surface	**Series**				**Wet**			
	Less than 48.28 km/h		More than 48.28 km/h		Less than 48.28 km/h		More than 48.28 km/h	
	From	To	From	To	From	To	From	To
Cement								
New, Sharp	0.80	1.20	0.70	1.00	0.50	0.80	0.40	0.75
Travelled	0.60	0.80	0.60	0.75	0.45	0.70	0.45	0.65
Traffic Polished	0.55	0.75	0.50	0.65	0.45	065	0.45	0.60
Asphalt or Tar								
New, Sharp	0.80	1.20	0.65	1.00	0.50	0.80	0.45	0.75
Travelled	0.60	0.80	0.55	0.70	0.45	0.70	0.40	0.65
Traffic Polished	0.55	0.75	0.45	0.65	0.45	0.65	0.40	0.60
Excess Tar	0.50	0.60	0.35	0.60	0.30	0.60	0.25	0.55

Gravel								
Packed, Oiled	0.55	0.85	0.50	0.80	0.40	0.80	0.40	0.60
Loose	0.40	0.70	0.40	0.70	0.45	0.75	0.45	0.75
Grass	0.45	0.45	0.45	0.45	0.45	0.45	0.45	0.45
Cinders, Packed	0.50	0.70	0.50	0.70	0.65	0.75	0.65	0.75
Rocks, Crushed	0.55	0.75	0.55	0.75	0.55	0.75	0.55	0.75
Ice, Smooth	0.10	0.25	0.07	0.20	0.05	0.10	0.05	0.10
Snow								
Packed	0.30	0.55	0.35	0.55	0.30	0.60	0.30	0.60
Loose	0.10	0.25	0.10	0.20	0.30	0.60	0.30	0.60

The values for gravel, grass, crushed rocks, ice, and snow in Table 1 are of significant interest to this thesis work, as they represent potential surfaces that can be used off-road by a military armoured vehicle. Of note, the impacts of climbing and downhill driving on hilly terrain also need to be considered and accounted for in the vehicle model.

2.1.3 Military Vehicle Considerations

An element that makes this work more of a niche study is the focus on the military application of the vehicle model. While civilian vehicles are often studied under the lens of maintaining a competitive edge in a capital market to make a profit, military vehicles are government-owned and government-operated; they are not designed to make a profit and are funded by taxpayer dollars. While research on civilian vehicles also focuses on improving vehicle performance, such as improving fuel economy and reducing greenhouse gas (GHG) emissions, this takes on a different meaning for the military. The focus of military vehicle performance is further defined by mobility, lethality, survivability, and sustainability; this will be covered further under the doctrine section.

Scenario Definition

Several different potential scenarios could apply to the design and implementation of a ‘green’ military armoured vehicle model. This work focuses on one such scenario that uses the advantages of an FCEV, as was highlighted in the research motivation section. The reduced noise and thermal profiles offered by fuel cell systems serve as passive protection that enhances vehicle survivability in the form of reduced detection by an adversary. This work will look at

a military armoured vehicle undergoing simulated performance conditions where the advantages of an FCEV would be highlighted: off-road movement at nighttime, under blackout conditions. Blackout conditions are when the vehicle does not use its lights - they are either turned off or covered by something such as tape, so that it may reach its destination undetected. Travelling off-road is also common for military vehicles for reasons of reduced detection and reduced risk of threat. During a time of conflict, roads are a strategic asset closely monitored, guarded, and even trapped with objects such as improvised explosive devices (IEDs). Therefore, it is essential to factor in an off-road component to the operation profile of the vehicle model.

Use of Doctrine

Given that data loggers will not be useful in this work for defining an operation profile, it must fall to military doctrine to provide guidance. Regarding vehicle mobility, the reference [4] provides recommended vehicle speeds based on different conditions. In particular, for an off-road move at night in blackout conditions with good weather conditions, the recommended speed is 15 - 20 km/h for a wheeled armoured vehicle, based on the quality of the off-road trail. While there are typical halts programmed into vehicles that undergo road movement as a means of traffic control and timing discipline, these are of little value to emulate in a vehicle model and should not be incorporated into the model design. In terms of determining the distance for the vehicle to travel, that will vary significantly based on the theatre of operation and the nature of the movement. Based on the author's military training and experience, 20 kilometres would be a rough average distance for a convoy to travel. When it comes to off-road action, it would make sense not to travel further if it can be avoided, given logistical considerations such as breaking down and requiring repairs from the unit's CSS element. Another consideration is that the Unit, the smallest group capable of independent operations over long periods, is supposed to be self-sufficient for 72 hours [11]. This rule does not simply mean 72 hours' worth of driving, and it covers all aspects of logistics such as the unit's fuel, food, and spare parts, to name a few pertinent considerations. Therefore, it is not unreasonable to assume an operational path length of approximately 20 kilometres.

2.2. Application of a Fuel Cell Electric Vehicle Powertrain with Rule-Based Control

2.2.1 Architecture

The powertrain architecture for an FCEV most commonly includes a PEM fuel cell system, an

electric motor/controller, a final drive, a power converter, electrical accessories and an electric ESS. The ESS commonly consists of a rechargeable battery pack, an ultracapacitor pack, or a combination of both, known as a hybrid energy storage system (HESS). Rechargeable batteries have much higher energy capacity, while ultracapacitors have the advantages of rapid charging and discharging, long operation life and temperature insensitivity. An HESS gets the benefits of both at the trade-off of increased complexity. For illustrative purposes, Figure 1 from [8] denotes one possible powertrain configuration for an FCEV.

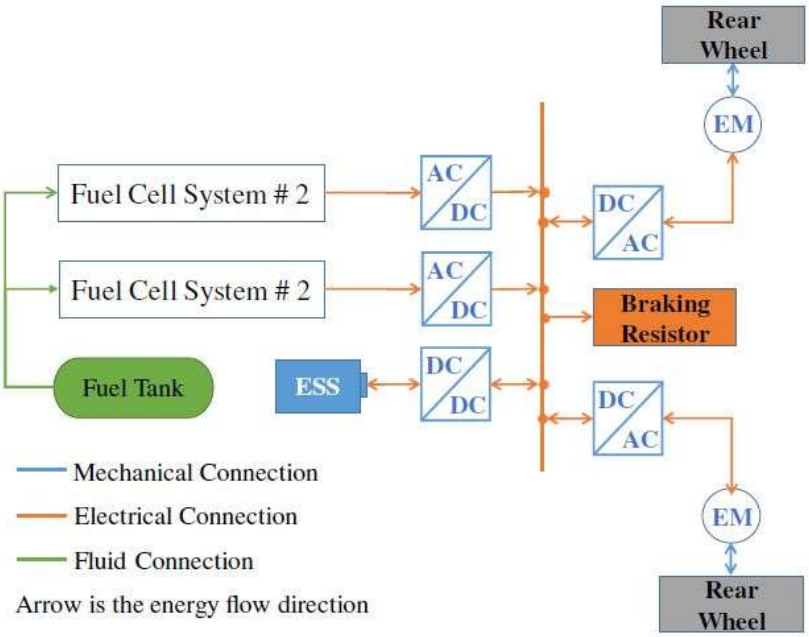

Figure 1: FCEV powertrain configuration, representing a hybrid electric mining truck [8]

In the above referenced diagram, the two fuel systems form the vehicle's fuel converter, which provides power to a power converter that connects to the electric motors that provide torque to the wheels. The ESS can both receive power from the regenerative braking from the wheels and provide power to the electric motors either by itself or in parallel with the fuel cell systems.

2.2.2 HESS Topology

There are three different topologies regarding the HESS: passive parallel, semi-active, and fully active. Passive parallel topology combines both the battery and ultracapacitor without using an electric converter such as a DC-DC converter. Advantages include the lower cost with a simple implementation, at the trade-off of the ultracapacitor not being used to its full potential, acting essentially as a low pass filter. The semi-active topology has the battery connected directly to

the powertrain. The ultracapacitor has a DC-DC power converter to act as a buffer between the ultracapacitor and the remainder of the power bus. Advantages include more efficient use of the ultracapacitor, with a wider voltage range and rapid power charging and discharging as needed by the system, less expensive and more efficient than a fully active topology. Semi-active topologies are the most common configuration used. The ultracapacitor is typically controlled to cover the peak power demand asked of the system, thus reducing power demand on the battery and extending battery life. In a fully active topology, both the battery and the ultracapacitor are connected to their own independent DC-DC power converter. The topology offers the advantage of fully decoupling the battery and ultracapacitor from the power bus and having more control over the voltage ranges, offering increased energy management options and flexibility. The drawbacks of this topology include increased complexity and cost and reduced energy efficiency due to losses experienced from both DC-DC power converters [12]. Figure 2 from [12] illustrates the semi-active HESS topology as described.

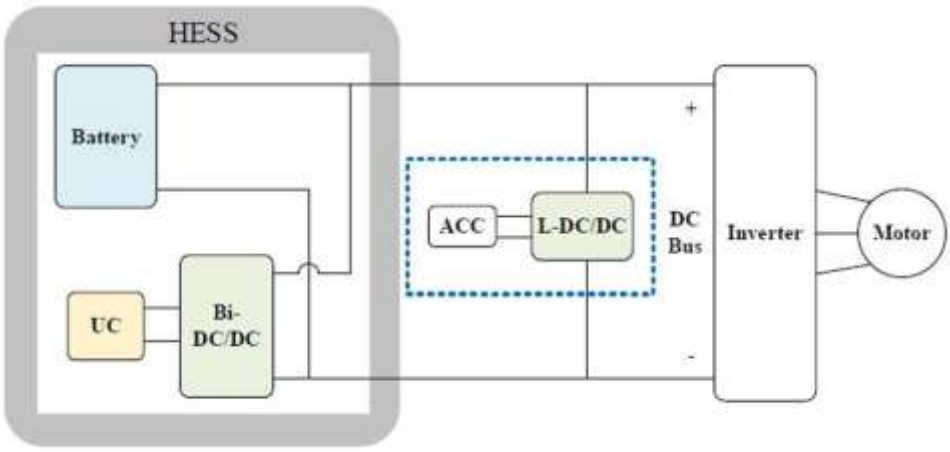

Figure 2: HESS semi-active topology [12]

The box highlighted by dashed blue lines in Figure 2 contains the vehicle's electric accessories connecting to the power bus via a low voltage DC-DC power converter, which is not part of the HESS topology but is still connected to the same power bus. One of the additional complexities of implementing a HESS is that it requires a controller to manage current throughput. It provides optimal use of the energy management system at every time step when running the model. The model from [8] uses dynamic programming to evaluate the optimal power demand of the battery and ultracapacitor at every time step. This arrangement leads to a disadvantage of using a HESS in a vehicle model, as dynamic programming involves minimizing an energy path across multiple possibilities at every time step, resulting in a computationally expensive model to solve. When nesting the energy management optimization

within the optimization function that seeks to minimize life cycle costs, the increased time that is taken to solve the model gets further amplified.

2.3. Vehicle Operation Costs

One of the responsibilities of the Government of Canada is to manage departmental budgets provided by taxpayer dollars, and the Department of National Defence (DND) is no exception to this responsibility. The Assistant Deputy Minister of Materiel (ADM (Mat)) is the branch of DND that manages capital crown projects and in-service support (ISS) of fielded equipment fleets, part of which involves life cycle material management (LCMM). LCMM includes monitoring the remaining useful life (RUL) of the equipment fleet, which is determined through usage and wear of equipment parts. For vehicle fleets, powertrain components are among the more expensive vehicle parts that largely determine the vehicle's RUL; in the case of an FCEV, that includes examining degradation costs associated with the fuel cell system and the ESS.

2.3.1 Fuel Consumption Cost

Same as all conventional energy converters, a PEMFC consumes fuel to generate propulsion power. Instead of gasoline or diesel, hydrogen fuel needs to be provided. As FCEVs are not yet widely used by the public, data involving fuel costs for hydrogen fuel is limited in nature. California is a location with enough FCEV usage that the California Energy Commission releases an annual report on the development of hydrogen infrastructure in their state. Based on their 2019 report, the average cost of hydrogen fuel per kilogram is $16.51 (USD) [13]. At the time of writing this work, the value of hydrogen fuel in Canadian dollars would therefore be $21.06 per kilogram.

2.3.2 Cost Associated with Powertrain Component Performance Degradation

Within the powertrain system of an FCEV, two key components, PEMFC and Li-ion battery in the electric ESS, contribute to a large proportion of the investment and replacement costs with a relatively short operational life. The performance degradation of PEMFC and Li-ion batteries determine their actual working life, requiring special consideration during the design and control development of the powertrain system.

PEMFC Performance Degradation

The work that described the powertrain architecture of fuel cell load-haul-dump (LHD) vehicles from [12] also provided a costing structure for the vehicle's fuel, as well as the performance degradation for both the fuel cell system and battery pack, outlined below.

$$Q_{\mathrm{FC}} = \frac{2C_{\mathrm{FC}}P_{\mathrm{nom}}}{\Delta V/\left(\xi_{\mathrm{low}}t_{\mathrm{low}} + \xi_{\mathrm{high}}t_{\mathrm{high}} + \xi_{\mathrm{chg}}\eta\right)} \tag{2.1}$$

Where Q_{FC} is dollar-cost from degradation loss, C_{FC} is the PEMFC manufacturing cost per unit power, P_{nom} is the nominal power from the fuel cell system, ΔV is the maximum allowable voltage degradation of the fuel cell system, ξ_{low} and t_{low} represents the degradation value and time when the fuel cell is idling (defined as being turned on and up to 10% of the fuel cell systems' maximum power), ξ_{high} and t_{high} represent degradation value and time spent under high power load (defined as using 90% of the fuel cell systems' maximum power), ξ_{chg} represents the degradation value of a dynamic load (defined as when the fuel cell systems switch from idle to its rated power), and η represents the number of times the fuel cell systems are subjected to a changing load. What works well with the equation from [12] is that models designed in software applications such as MATLAB/Simulink are able to capture the simulation runtime, which can be fed back to the script being executed and calculate the degradation costs in post-processing after the model has finished running.

Li-ion Battery Performance Degradation

Similarly, the same paper [12] expressed a degradation cost equation for batteries as well, outlined in the equations below.

$$Ah_{\mathrm{allow}} = \sqrt[z]{0.2/\left(A\exp\left(-\frac{E_{\mathrm{a}} + B\ C\_Rate_{\mathrm{cycle}}}{R\ T_{\mathrm{batt}}}\right)\right)} \tag{2.2}$$

$$Q_{\mathrm{batt}} = C_{\mathrm{batt}}E_{\mathrm{nom}}\left(\frac{Ah_{\mathrm{cycle}}}{Ah_{\mathrm{allow}}}\right) \tag{2.3}$$

Where in (2.2): Ah_{allow} is the maximum allowable battery ampere-hour value, A is the pre-exponential factor, E_{a} is the activation energy, R is the gas constant, T_{batt} is the absolute temperature, C_Rate_{cycle} is the discharge rate of the cycle, B is the compensation factor of the discharge rate, and 0.2 represents the maximum allowable battery degradation of 20% from its ideal value. For equation (2.3): Q_{batt} is the degradation cost of the battery, C_{batt} is the cost of the battery per kWh, E_{nom} is the battery nominal energy capacity, Ah_{cycle} is the value of

ampere-hours from the model's cycle, and Ah_{allow} is the value calculated from the previous equation.

One of the challenges that will be faced when calculating degradation costs for the model is that the model will be constrained to designs where the parameters for the battery are already known from experimental values. This is a constraint because these values are determined from experimental data, cannot be calculated from scratch, and most often, companies keep these values private as part of their intellectual property. This means that better batteries may exist that could better benefit the vehicle model's performance but cannot be used due to insufficient data required by the model. Examples of such values are the battery's pre-exponential factor, activation energy, and compensation factor for discharge rate. This problem is less so the case for the model's fuel cell systems because those values can be calculated as a result of running the model and writing those values to a workspace where they can be determined in post-processing.

2.4. Summary of Literature Review

At the time of writing, there are no models of military armoured vehicles with fuel cell powertrain configurations, nor are there methods for creating military operation profiles without the use of data loggers. This means that a novel approach will be required to solve these problems. There does exist, however, literature centred around heavy-duty vehicles such as mining trucks, meaning there are comparable models that can serve as the base framework in developing a military armoured vehicle model such that one does not need to be designed from scratch. Degradation calculations exist for fuel cell systems and battery packs for the vehicle's powertrain; however, a constraint has been identified early on in the form of requiring specific battery parameters that can only be found through experimental values of actual batteries in a lab.

Chapter 3. Design of a Military FCEV through Modeling and Simulation

3.1. Operation Profile Modeling

In creating an operation profile, it is essential to ensure parameters such as the environmental factors, pathway travelled, and speeds used by the vehicle are realistic, meaning that collaboration with the end-users of the vehicle should take place. For this work, the end-users of the vehicle are the Canadian Army element of the Canadian Armed Forces. The author is an active member of the Canadian Army with 15 years of service as an officer of the Royal Canadian Electrical Mechanical Engineering (RCEME) Corps, which offers the unique position of having access to the military knowledge and access to the resources and points of contact not typically afforded to an individual outside of the organization. Whether due to government protection of sensitive information or the niche nature of the subject matter, and given there is little academic work publicly available on the subject matter, having the resources previously mentioned will serve as the foundational basis for constructing an operation profile from scratch.

3.1.1 Collaboration with the Canadian Army

The pathway for the vehicle model used in this work was created in collaboration with the combat engineers from the 4th Engineering Support Regiment (4 ESR) in Canadian Forces Base (CFB) Gagetown, New Brunswick. CFB Gagetown has one of Canada's largest Range Training Areas (RTAs), making it a suitable location to create a vehicle pathway. The nature of combat engineers' work makes them uniquely suitable end-user clients with which to collaborate. Combat engineers are responsible for ensuring mobility for land forces. In order to perform these duties, they use a variety of vehicles and equipment to shape terrain, build bridges, clear obstacles/mine-sweep, generate maps, and perform geospatial terrain analysis, amongst other responsibilities. Combat engineers are therefore career subject matter experts (SMEs) for determining movement paths and in operating armoured vehicles. Both are critical to this work in forming a viable operational pathway.

For this work, the combat engineers of 4 ESR took the requirements the author provided them and created a planning map that contains a pathway for an armoured vehicle, which can be found in Annex A. The requirements were to create a path an armoured vehicle would

realistically travel for approximately 20 kilometres off-road on terrain that has a changing elevation profile. From this map, an electronic 'shapefile' of the vehicle's pathway can be created that can be overlaid onto a raster data representation of the map, from which distance and elevation data can be extracted. Initially, the geo-mapping software Quantum Graphing Information System (QGIS) was used to extract a distance and elevation profile but ran into difficulties merging multiple mini maps into a mosaic that made the resulting data unusable, producing unrealistic and fluctuating values for elevation. Using the Universal Transverse Mercator (UTM) coordinate system, a series of UTM maps in the form of '.TIFF' files were formed to create a mosaic raster representation of CFB Gagetown to create an electronic operation profile. Unfortunately, merging the '.TIFF' files created an unrealistic fluctuation in elevation data values that made the profile unusable. To address this, the vehicle's pathway in the form of a '.kml' file was loaded into Google Earth Pro, which was able to convert the file into a distance and elevation profile. While the distance values were extracted from Google Earth Pro in the form of GPS coordinates and a series of trip segments, separate software from [14] was required to return a text file that matched elevation values to the corresponding GPS trip segments.

3.1.2 Application of the Haversine Equation

In order to convert GPS coordinates into distance values between trip segments, the Haversine equation was used. When distances are approximately up to a maximum of 20 kilometers, the earth can be considered 'flat,' and as such the Pythagorean Theorem can be used to calculate distance travelled between horizontal distance and vertical elevation data. While this vehicle model falls within the upper bound of qualifying to use flat earth calculations, this creates obvious model constraints for creating and using other operation profiles with larger distances. The Haversine equation treats the earth as a sphere, calculating the great circle distance between two points of longitude and latitude. While it is recognized that the earth is ellipsoidal and not spherical, the operational range of a vehicle is sufficiently short enough that resulting errors are minimal, such that more complex and computationally intensive calculations for improved accuracy are not required [15]. The Haversine method of calculating distance is outlined below.

$$\mathrm{hav}\left(\frac{d}{r}\right) = \mathrm{hav}(\varphi_2 - \varphi_1) + \cos(\varphi_1)\cos(\varphi_2)\mathrm{hav}(\lambda_2 - \lambda_1) \tag{3.1}$$

Where d is the distance the vehicle travels, r is the radius of the earth, φ_1 and φ_2 are the latitude

coordinates of the origin and destination points of a trip segment respectively, and λ_1 and λ_2 are the longitude coordinates of the origin and destination points of a trip segment, respectively.

$$\text{hav}(d/r) = \sin^2\left(\frac{d/r}{2}\right) = \frac{1-\cos(d/r)}{2} \tag{3.2}$$

$$d = \sum_{n=1}^{N}\left(2r\ x\ \arcsin\left(\sqrt{\sin^2\left(\frac{\varphi_{2,n}-\varphi_{1,n}}{2}\right)+\cos(\varphi_{1,n})\cos(\varphi_{2,n})\sin^2\left(\frac{\lambda_{2,n}-\lambda_{1,n}}{2}\right)}\right)\right) \tag{3.3}$$

Where *n* represents an index of the trip segment being evaluated, and *N* is the total number of trip segments in the operation profile.

The number of trip segments used in the operation profile was created by tracing over the '.kml' file on the Google Earth Pro overlay. The total sum of the distances of the trip segments is calculated from (3.3), forming the horizontal distance of the operation profile. The elevation profile extracted from software from [14] has elevation values corresponding to the GPS waypoint coordinates. Then, if distance and elevation can be considered as x-y coordinates on a Cartesian plane, the distance and road gradient in degrees can be calculated using (3.4) and (3.5), respectively.

$$distance = \sum_{n}^{N}\left(\sqrt{(horizontal\ distance)^2+(elevation)^2}\right) \tag{3.4}$$

$$road\ gradient = \sum_{n}^{N}\tan^{-1}\left(\frac{elevation}{horizontal\ distance}\right) \tag{3.5}$$

With distance and elevation determined for the operation profile, there needs to be an associated speed that corresponds with those values when the model is running. Because there is no data logger to track speed, instead, army doctrine must be relied upon. Given that the off-road paths in the CFB Gagetown RTA are in good usable condition, based on doctrine, in blackout conditions, a constant 15-20 km/h is the recommended travel speed [4]. This work has chosen to implement the upper bound of 20 km/h for the vehicle model, as the model should be subjected to the most rigorous conditions feasible for the scenario. While road movements typically involve planned halts while on the move, there is little benefit to incorporating turning off the vehicle and sitting still for half an hour in the model. Thus, for the purposes of developing the operation profile, the model turns on from rest, accelerates to reach the designated speed, and then brakes to a stop once the destination is reached. Table 2 lists the remaining parameters that form the operation profile the vehicle model is subjected to, which

are considered average values in North America, where the operation profile was created.

Table 2: Operation profile parameters

Variable	Value (Units)
Ambient Temperature	20 (°C)
Ambient Pressure	101300 (Pa)
Gravitational Constant	9.81 (m/s^2)
Air Density	1.1985 (kg/m^3)
Air Humidity Ratio	50 (%)

These parameters get entered into an initialization script in MATLAB, which then gets used in Simulink systems and subsystems calculations. More specifically, the values in Table 2 are primarily used to calculate propulsion force loss due to drag, with temperature also having an impact on fuel cell and ESS calculations.

3.2. Modelling of Military FCEV

The modelling of a functional vehicle consists of three major components:

Operation profile of the vehicle

The operation profile model defines the use pattern of the vehicle, on which the performance, fuel consumption and emissions are measured, and proper powertrain system configuration and component size are determined.

Vehicle dynamics model

The vehicle dynamics model captures and predicts the dynamic performance behaviour and energy efficiency of the vehicle. Furthermore, fuel consumption and emissions can be predicated based upon the power loss calculation using this model.

Powertrain system model

The model forms the vehicle powertrain with defined powertrain architecture, powertrain components with given sizes, and the powertrain system's power control and energy management strategies.

The combination of the vehicle dynamics model and its powertrain system model is called the vehicle model in this work. This work's primary focus and original innovation is developing the operation profile and determining the operational cost of the armoured military FCEV due to fuel consumption and powertrain degradation. While 'turn-key' solutions exist via software

applications such as ADVISOR and Autonomie, they are inadequate for the purposes of this work because many powertrain components are outdated, and the models are tailored for civilian and not military application. Therefore, for this work, a customized model based design is required. That being said, the vehicle dynamics and powertrain system models of the armoured military vehicle were not created completely from scratch. Instead, these models produced by the Clean Transportation team at the University of Victoria for similar heavy-duty vehicles [16] were adopted as the framework from which to form the modified armoured military vehicle model. The focus of discussion in this work will be the general overview of how these models work and the parts of the model that were modified to turn it into a representation of an armoured vehicle.

3.2.1 Vehicle Model Overview

The vehicle model has four major subsystems: vehicle (vehicle dynamics and powertrain system), environment, driver, and controller, illustrated by Simulink below. Each subsystem will be broken down one level further, following the high-level overview.

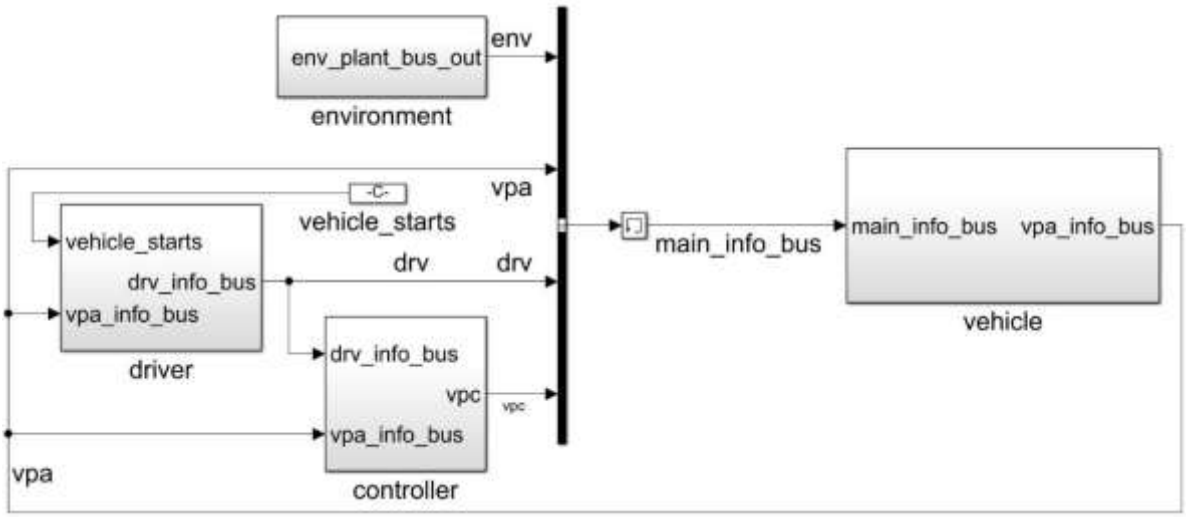

Figure 3: High-level overview of the vehicle model

In the middle of Figure 3 is the main signal information bus, which transports all the signals between the subsystems. A block containing a constant signal informs the driver subsystem that the vehicle is turned on, which sends the driver subsystem information such as the operation profile, driver response time, and acceleration/braking input to the vehicle controller. The vehicle controller takes the inputs from the driver subsystem, and at each time step, calculates the required torque and power outputs to match the demand from the operation profile, sending these signals to the plant, which in this model is the vehicle to action. The vehicle subsystem

actions the input from the other subsystems and provides continuous feedback to the other subsystems as the model continues to run. There is a block in between the signal bus and the vehicle that is called a 'Memory Block', seen in Figure 3 as the block with the rectangular arrow. Its purpose is to offset signals by a time step when the model is running to prevent an algebraic loop from occurring. An algebraic loop is when a signal loop exists with only direct feedthrough blocks within the loop, where you would need the output in order to calculate the input. By offsetting the signals by a time step, it enables the solver to calculate the output without crashing the model with a critical error.

3.2.2 Vehicle Model Subsystems

Environment Subsystem

The environment subsystem contains all the constants from Table 2, as well as the road grade table used by the vehicle model. In addition to Table 2, the parameter called 'Temperature Mode' takes the temperature and applies it to design and manage fuel cell cooling.

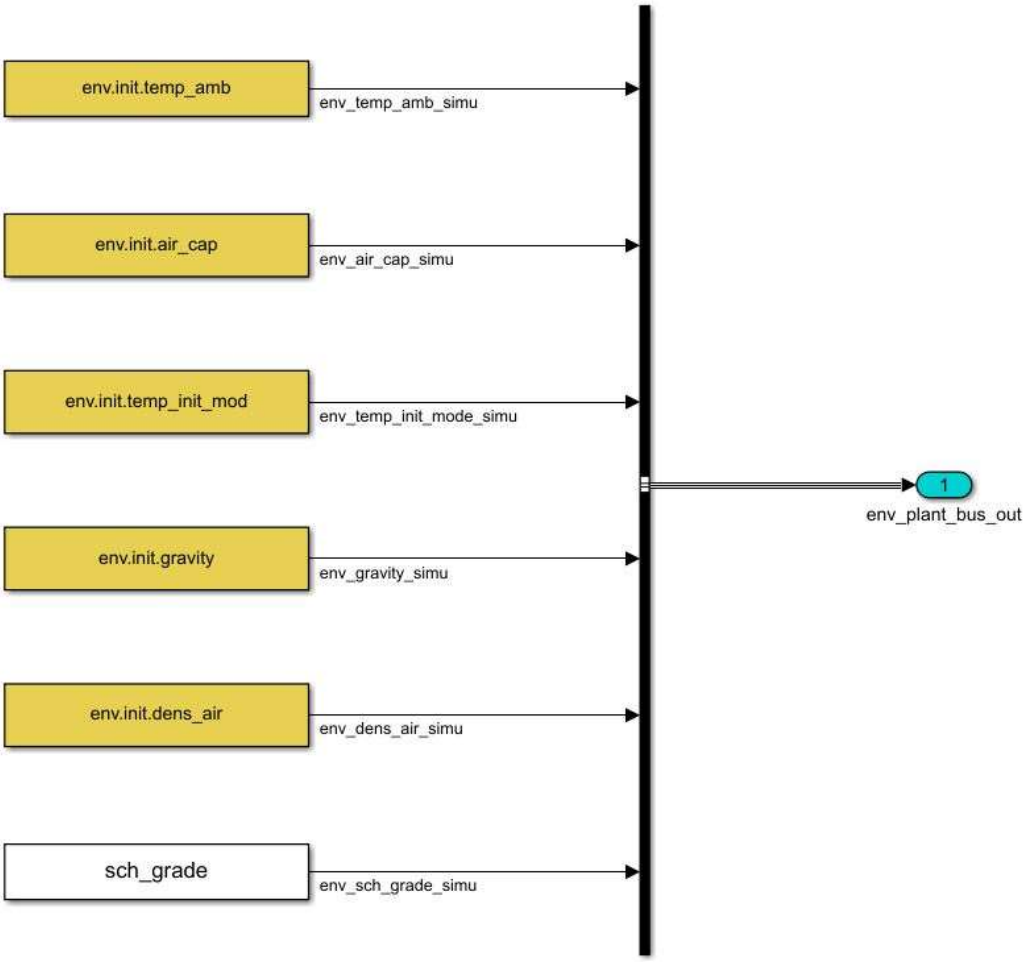

Figure 4: Environment subsystem

Figure 4 is very similar to Table 2 in that it contains the environmental parameters used to calculate various factors in the vehicle model such as propulsion force loss, which includes the addition of the grade schedule used to also calculate propulsion force loss.

Driver Subsystem

The driver subsystem takes the speed and elevation inputs and turns it into a torque demand signal sent to the controller. In an ideal world, the plants in the vehicle model would perfectly match as output what the torque demand sent in as input, but plant losses and system complexity can lead to errors which require both oversight and correction as needed. To correct for error, a PI controller measures the error between the demanded speed from the operation profile and the linear chassis speed from the vehicle plant and corrects the error at each time step. Because the operation profile is pre-determined from start to finish, an array is imported with the demanded vehicle torque that propels the vehicle, which is used in conjunction with the PI controller to send the demanded torque to the brake and accelerator controllers. Figures 5 and 6 illustrate how the PI controller and torque array are combined.

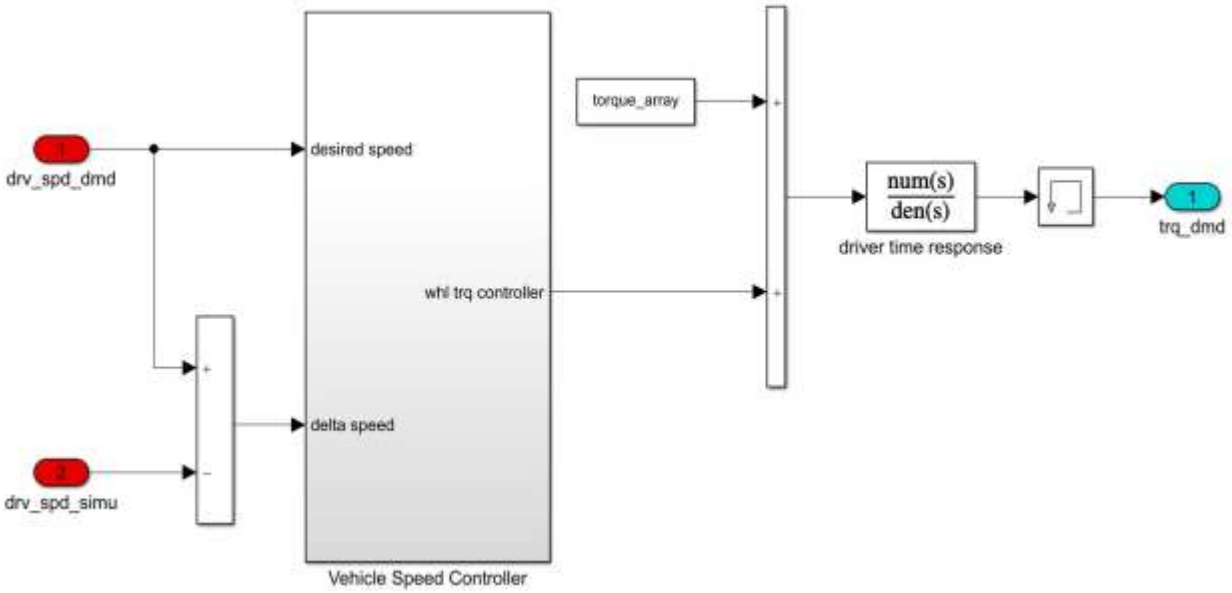

Figure 5: Vehicle torque demand estimator subsystem

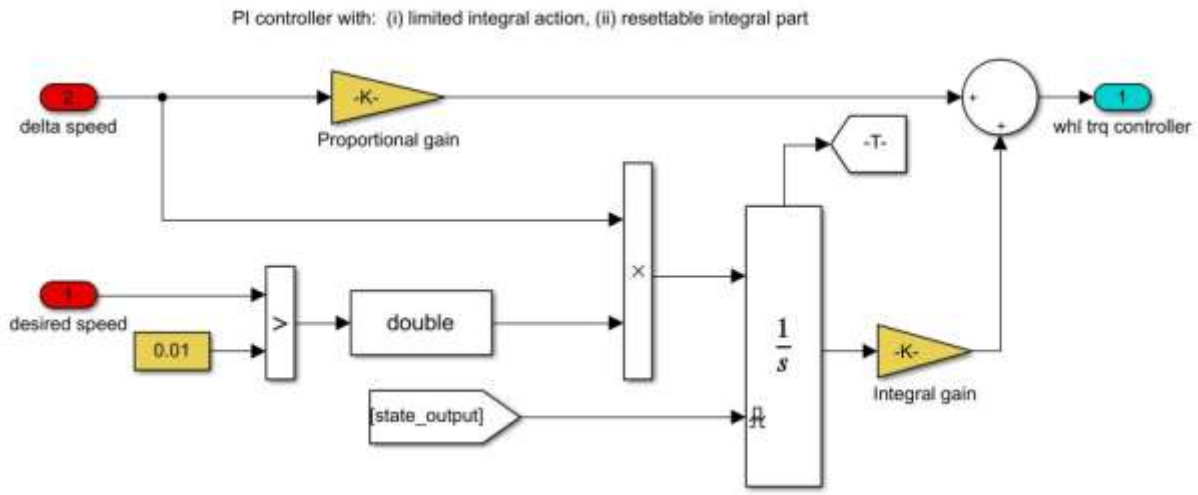

Figure 6: Vehicle speed controller subsystem

One additional component to the torque demand estimator seen in Figure 5 is taking the driver delayed response into account, which adds a 0.2 second delay to the driver either applying the brake or the accelerator pedal, representing the brief delay in driver response in real life to driving. The torque array is created based on the speed and elevation from the operational profile and the resistance experienced by the vehicle. This vehicle model experiences the following forces: the force of propulsion (F_P), the force of gravity (F_G), drag resistance (F_D), and rolling resistance (F_R). The equations below were used to construct the torque array.

$$a = \frac{dU}{dt} \tag{3.6}$$

Where a is acceleration, and $\frac{dU}{dt}$ is the change in speed over time.

$$F_P = m\,a \tag{3.7}$$

Where F_P is the propulsion force, and m is the vehicle mass.

$$F_G = m\,g\,\sin(\theta) \tag{3.8}$$

Where F_G is the force due to gravity, g is the gravitational constant, and θ is the angle of the road grade.

$$F_D = \frac{1}{2}\,\rho\,C_D\,A\,U^2 \tag{3.9}$$

Where F_D is the force due to drag, ρ is the air density, C_D is the drag coefficient of the vehicle chassis, A is the frontal area of the vehicle chassis, and U is the vehicle's linear velocity.

$$F_{RR} = m\,g\,\cos(\theta)(k_0 + k_1\,U) \tag{3.10}$$

Where F_{RR} is the force due to rolling resistance, k_0 is a zero-order rolling coefficient, and k_1 is a first-order rolling coefficient.

$$F_{\mathrm{Losses}} = F_{\mathrm{G}} + F_{\mathrm{D}} + F_{RR} \tag{3.11}$$

Where F_{Losses} is the sum of all force losses.

$$F_{\mathrm{dmd}} = F_{\mathrm{P}} + F_{\mathrm{Losses}} \tag{3.12}$$

Where F_{dmd} is the force demanded by the vehicle controller in order to overcome force losses and meet the demanded vehicle speed.

$$T_{\mathrm{dmd}} = F_{\mathrm{dmd}}\, r \tag{3.13}$$

Where T_{dmd} is the required torque at the wheels to meet the demanded vehicle speed, and *r* is the radius of the vehicle wheels. The resulting torque demand gets sent to either the brake or acceleration controller, depending on whether the vehicle is speeding up or slowing down, based on the input from the operation profile.

Vehicle Controller Subsystem

While there are numerous subsystems in the vehicle model exercising some form of control of signals that get sent to the plant for action, the vehicle controller can be considered the 'brain' of the vehicle model, making decisions regarding the state of the vehicle at every time step. The goal of the vehicle controller subsystem is to ensure that the vehicle is providing adequate power to the vehicle at each time step and not providing an excess of power to the vehicle (which reduces fuel efficiency). The vehicle controller manages multi-mode power split settings that alternate between 'Electric Only' (EV) mode, 'Hybrid Electric Vehicle' (HEV) mode, and a 'Performance' mode, with sub-states existing within those states. This controller also accounts for when the vehicle is idling. To illustrate the controller logic for propulsion, Figure 7 shows the different states within Stateflow controlling the vehicle.

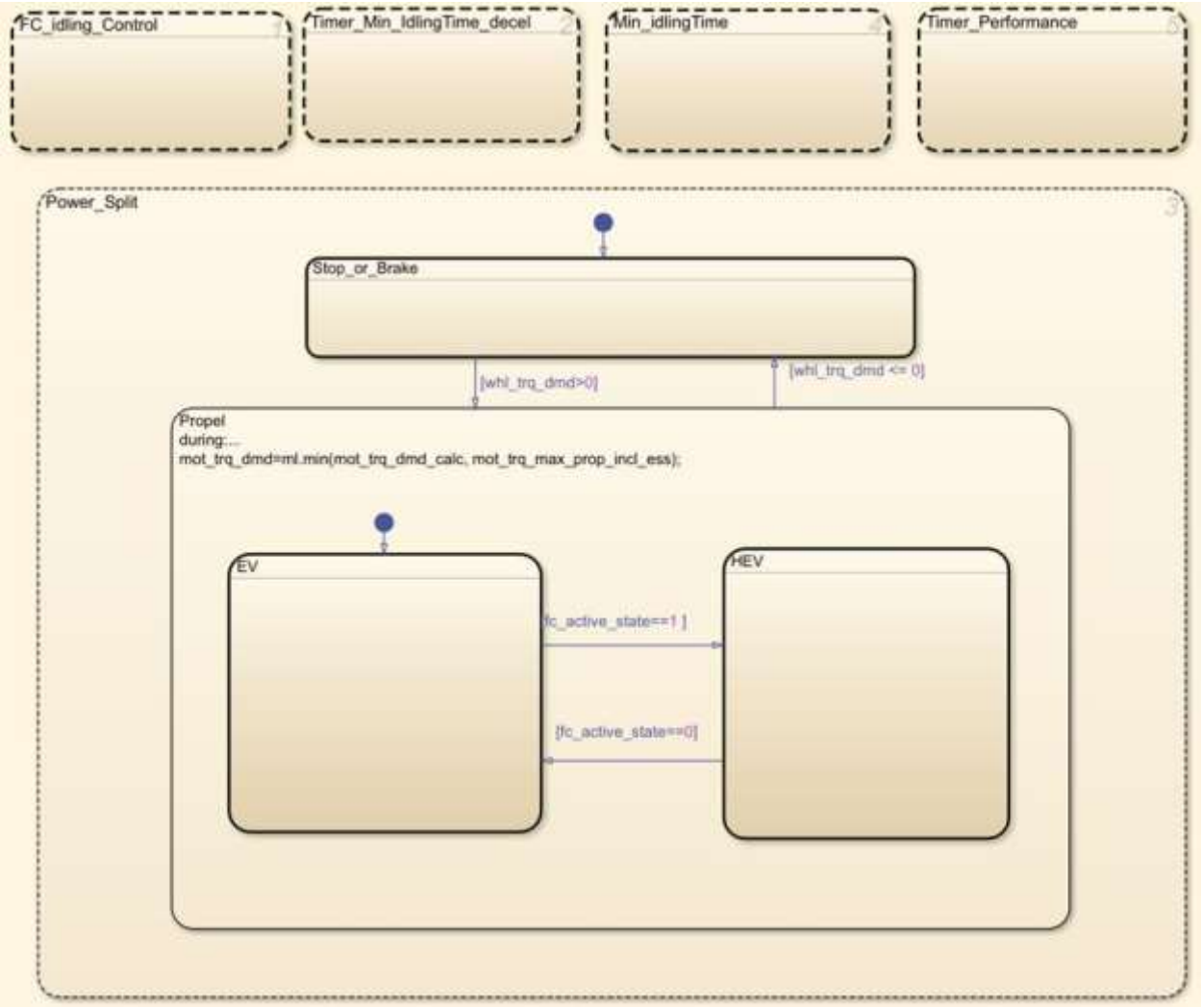

Figure 7: Stateflow controller for vehicle propulsion

The solid blue circles seen in Figure 7 show the initial states the vehicle starts in. For this vehicle model, the vehicle starts at rest as well as in EV mode, meaning it only uses the ESS to power vehicle propulsion while in that state. The vehicle engages in propulsion when the torque demand at the wheels is assessed to be greater than 0 and applies brakes/stops when the torque demand is less than or equal to 0. When the vehicle's power demand exceeds what the ESS can supply, the fuel cell systems get turned on, and the vehicle shifts from EV mode to HEV mode. HEV mode includes Performance mode as a sub-state, illustrated by Figure 8 for better understanding.

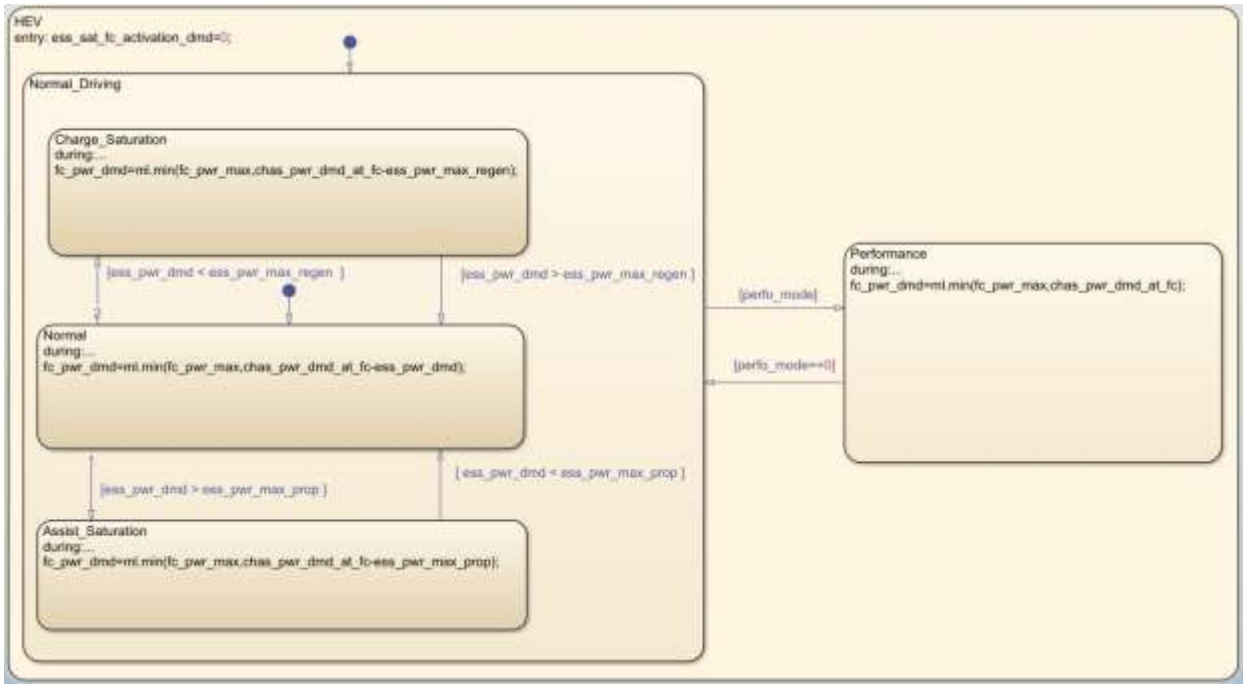

Figure 8: Stateflow controller subsystem for hybrid electric vehicle and performance mode

In Figure 8, the initial start points in this state are the 'Normal' sub-state within the 'Normal_Driving' state, which satisfies the system's power demand through the minimum value of either the fuel cell system's maximum power or the difference between the demanded power from the fuel cell system and the ESS. The power demand at the ESS determines the transition to the other sub-states. If the ESS power demand is less than available capacity to regenerate ESS power, then the sub-state transitions to 'Charge_Saturation,' where the fuel cell system charges the ESS at the rate of the difference between the ESS power demand and the ESS max regen rate. If, on the other hand, the ESS power demand is greater than the value of the ESS' max propulsion value, then there is a transition to the 'Assist_Saturation' sub-state, where the power provided to the system is the minimum between the maximum power at the fuel cell system and the difference between the fuel cell system and the ESS maximum power. Note that 'Performance' mode must be manually incorporated into the script of the vehicle model; it is not an automatic transition in Stateflow. This represents the button on a vehicle's user interface to press since performance mode is not a fuel-efficient mode to operate in. For the vehicle model in this work, 'Performance' mode is not used.

As ESS power demand plays an important role in the power management of the vehicle model, how ESS power demand is determined will be discussed in this section, with the remainder of the ESS design being discussed in the Vehicle section of the paper. ESS power demand is determined at each time step based on the ESS' state of charge (SOC), contained within a one-

dimensional (1-D) lookup table. The ESS power demand map was built as part of the vehicle model framework inherited from [16], shown below.

$$ESS_{\text{Dis\_max}} = \left(ESS_{\text{C\_Rate}}\right)\left(Modules_{\text{Par}}\right) \tag{3.13}$$

Where $ESS_{\text{Dis\_max}}$ is the maximum discharge current of the ESS, $ESS_{\text{C\_Rate}}$ is the battery charge rate, and $Modules_{\text{Par}}$ represents the number of battery modules in parallel.

$$ESS_{\text{Chg\_max}} = \left(-ESS_{\text{C\_Rate}}\right)\left(Modules_{\text{Par}}\right) \tag{3.14}$$

Where $ESS_{\text{Chg\_max}}$ is the maximum charge current of the ESS.

Table 3: ESS power demand logic, based on SOC range

ESS SOC Range (%)	ESS Power Demand Equation Used
0.1 - 20	$\left(ESS_{\text{Chg\_max}}\right)\left(Modules_{\text{Ser}}\right)$
20.1 - 60	$\left(ESS_{\text{Chg\_max}}\right)\left(Modules_{\text{Ser}}\right)0.5$
60.1 - 80	$\left(ESS_{\text{Dis\_max}}\right)\left(Modules_{\text{Ser}}\right)0.5$
80.1 -100	$\left(ESS_{\text{Dis\_max}}\right)\left(Modules_{\text{Ser}}\right)$

In this vehicle model, the target SOC to be maintained is 60%, this is why there is a scalar value of 0.5 affecting the charge and discharge rate around that 60% value, so that charge and discharge rates are slower around the target SOC, reducing the number of battery cycles and thus slowing battery degradation. The scalar value of 0.5 was chosen around the target SOC so that overshooting doesn't occur during management of battery charging and discharging, and the target SOC of 60% was selected such that the battery can still be useful during the application while also not draining entirely, thus seeking to extend its life while also still being able to use it.

Vehicle Subsystem

The vehicle subsystem is the plant of the model that actions the signals from the controller. The vehicle subsystem is broken into nine sub-subsystems: fuel cell, power converter 1, power converter 2, electric motor, final drive, wheels, chassis, electric accessories, and ESS. All sub-subsystems within the vehicle subsystem will have a brief overview of functionality, except the ESS. The ESS from the provided vehicle mode was replaced entirely during this work, requiring a more detailed description of its design.

Fuel Cell Sub-Subsystem: The fuel cell sub-subsystem takes the on/off signal as input and sends power as output. The type of fuel cell system used in the vehicle is the Proton Exchange

Membrane Fuel Cell (PEMFC) system, which uses hydrogen fuel and anodes/cathodes to enable the separated hydrogen electrons to be passed to an electrical circuit, thus generating electrical power. The hydrogen by-product mixes with oxygen to produce water out the vehicle's exhaust, and the model also accounts for the amount of hydrogen fuel consumed. Table 4 highlights the key fuel cell parameters used by the vehicle, Figure 9 shows the plant design of the fuel cell sub-subsystem.

Table 4: Fuel cell sub-subsystem key parameters [16]

Parameter Name	Value (Units)
Maximum Output Power	300000 (W)
Fuel Tank Volume	6.0414 (m^3)
Fuel Heating Value	1.2e8 (J/kg)
Fuel Density Value	0.018 (kg/m^3)
Maximum Efficiency	59.52 (%)
Number of Fuel Cells in System	2400
Nominal Voltage	0.7 (V)

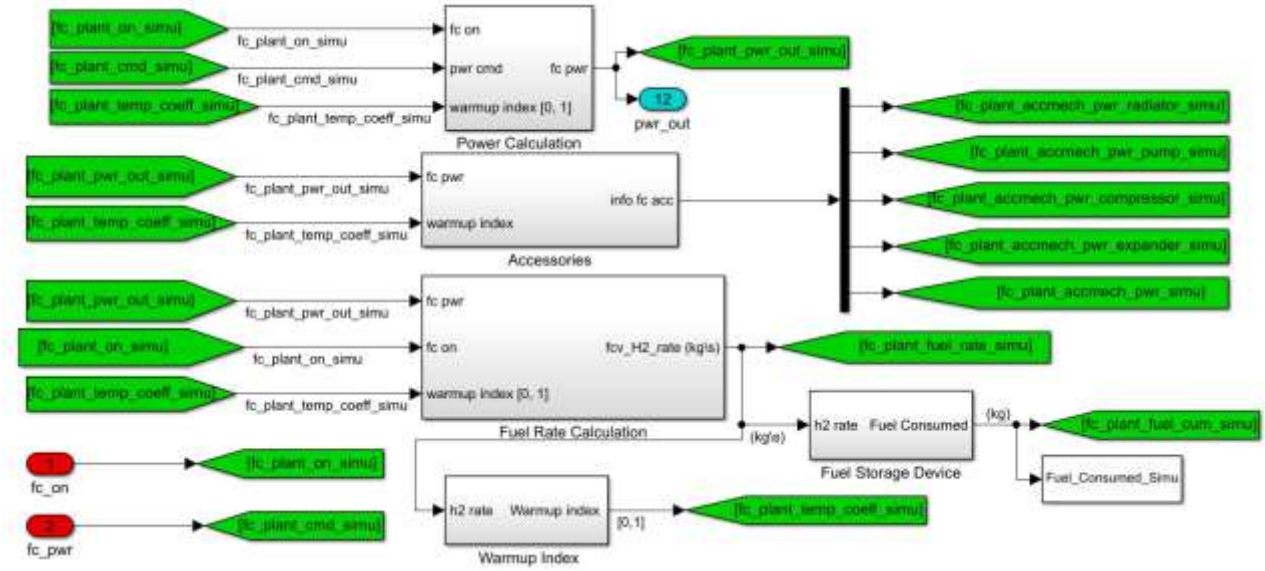

Figure 9: Fuel cell sub-subsystem plant breakdown

The power generated by the fuel cells is based on the evaluation of warmup and cool-down curves of the PEMFC temperature, which can be seen in Figure 9 via the 'warmup index' signal. As the focus of this work is on the design of the operation profile, further breakdown of temperature and its function on fuel cell performance is outside of the scope of this work. It can also be seen in Figure 9 that the hydrogen fuel consumed is captured by the sub-subsystem and sent to the MATLAB workspace for operation profile costing during post-process calculations.

Power Converters 1 and 2: The role of the two power converters is to regulate the voltage between powertrain components, ensuring there is voltage stability between subsystems. Power converter 1 sends DC voltage to the electric accessories, while power converter 2 regulates DC voltage and current between the fuel cell system and the ESS. Table 5 highlights the key parameters of power converters 1 and 2.

Table 5: Key parameters for power converters 1 and 2 [16]

Parameter Name	Value (Units)
Power Converter 1 Efficiency	100 (%)
Power Converter 2 Efficiency	97 (%)
Power Converter 1 Voltage Out	12 (V)
Power Converter 2 Voltage Out	300 (V)

Due to the complexities of evaluating power demand for electrical accessories and determining the associated losses at the power converter, the power converter for electrical accessories is assumed to be ideal.

Electric Motor: The electric motor takes voltage from the ESS and vehicle speed feedback from the final drive as input and provides motor torque to the final drive as output. For the vehicle model in this work, the initial electric motor was not powerful enough to propel the vehicle, so a "motor scaling factor" was introduced to find a solution for this. The motor scaling factor is a value used to scale the power and torque output such that the motor was capable of supporting vehicle model propulsion. The motor scaling factor was manually tuned until the error between the demanded speed from the operation profile and the actual speed from the model was within the accepted error of 2% during test runs. The test runs used an ESS configuration of 4x ESS modules in series and 4x ESS modules in parallel, which was considered 'middle of the road' for testing purposes; more information regarding ESS is covered in the ESS section. The section on ESS A scaling factor of 4 was applied to all original values, which means the output maps of all-electric motor parameters were multiplied by 4 to represent a more powerful electric motor. Table 6 highlights the key parameters of the electric motor after the scaling factor was applied. Figures 10 and 11 show the Simulink sub-subsystem overview and the motor efficiency map, respectively.

Table 6: Key parameters for the electric motor [16]

Parameter Name	Value (Units)
Minimum Voltage	250 (V)
Maximum Torque	750 (Nm)
Minimum Torque	-750 (Nm)
Maximum Current	500 (A)
Inertia	0.04 kg*m^2

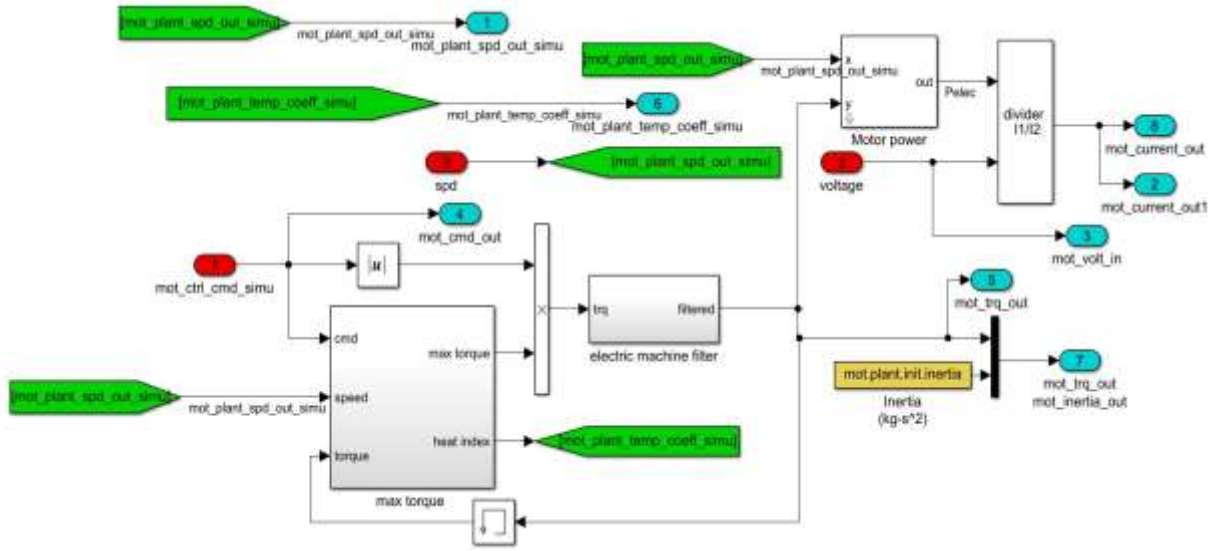

Figure 10: Electric motor sub-subsystem plant overview

It can be seen in Figure 10 that the demanded motor torque from the controller is the input that drives calculations for motor power based on motor speed and torque. Based on voltage input from the ESS, the motor current is calculated and then fed back into the system as an input for the ESS using

$$I = \frac{P}{V} \tag{3.15}$$

Where I is the motor current output, P is the power generated by the electric motor, and V is the input voltage from the ESS.

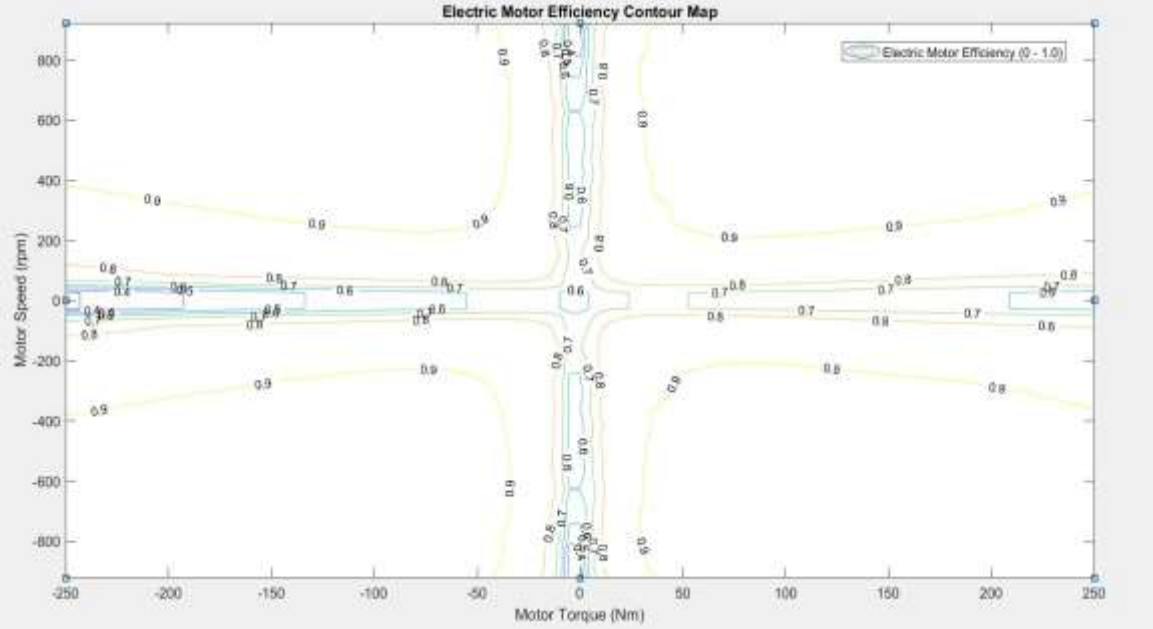

Figure 11: Electric motor efficiency contour map

Where the electric motor appears to be most efficient when the motor speed is approximately ± 400 rpm, and the motor torque is approximately ± 45 Nm; as both the motor speed and motor torque approach zero, motor efficiency drops within the range of 40% to 60% efficient.

Final Drive: The final drive takes the motor torque and inertia from the electric motor, as well as speed feedback from the wheels as input, and provides a torque with inertia values to the wheels, which propels the vehicle. The final drive ratio for the vehicle model is 15.0; the value was selected to be higher so that there could be more torque at the wheels at the trade-off of a lower top speed, which is appropriate for an armoured vehicle that requires more terrain versatility than its need to operate at high speeds.

Electric Accessories: Electric accessories include aspects such as air conditioning, vehicle fans, and the vehicle entertainment system. Due to the complexities of representing the dynamic values of electric accessories, this vehicle model's electric accessories have zero power draw.

Chassis: The vehicle chassis chosen in this model is a close approximation of the Tactical Armoured Patrol Vehicle (TAPV) acquired by the Canadian Armed Forces (CAF) in 2016. It is an approximation so that a vehicle model representing an armoured vehicle by the Canadian Army can be used while also not giving away exact technical specifications in a public forum. All information used has been pulled from online, public sources such as [17]. The chassis takes propulsion force from the wheels as input and outputs a linear speed that is used as feedback for other subsystems. Key parameters for the vehicle chassis can be found in Table 7, while Figure 12 shows an illustration of the TAPV as used by CAF, taken from [19].

Table 7: Key parameters for the vehicle chassis

Parameter Name	Value (Units)
Mass	18000 (kg)
Drag Coefficient	0.7
Frontal Area	7.12 (m^2)
Ratio of Weight in the Front	0.4
Length	6.31 (m)
Width	2.75 (m)
Height (with wheels)	3.225 (m)

Figure 12: The TAPV, illustrated driving off-road [18]

Figure 12 from [18], in addition to providing an image of what the vehicle model is representing, also serves as a reminder as to why the development of an operation profile is needed: the TAPV seen above is off-roading on terrain that would not be traversed by a typical civilian vehicle.

Wheels: The wheels used in this vehicle model take the final drive torque and inertia values as input, and output a force to the chassis to calculate linear vehicle speed. The wheels used in this vehicle model closely approximates the Michelin XZL 16.00R20 tires used by the TAPV. Table 8 highlights the key parameters for the vehicle wheels, and Figure 13 illustrates the tire being represented, taken from [19].

Table 8: Key parameters for the vehicle wheels

Parameter Name	Value (Units)
Mass (all wheels)	607.27 (kg)
Aspect Ratio	90
Wheel Radius	0.6604 (m)
Coefficient of friction	0.7

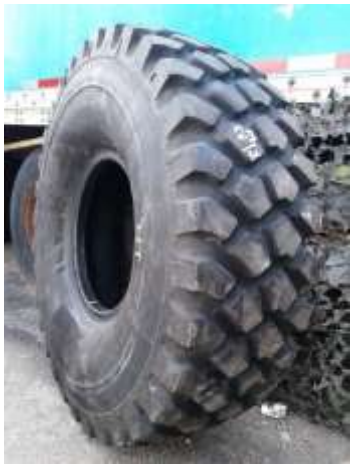

Figure 13: Michelin XZL 16.00R20 tire [19]

Electric Storage System: Given that the electric ESS sub-subsystem was replaced entirely from the original model so that battery degradation could be factored into powertrain costing, this section will be covered in more detail than the higher-level overview of the other powertrain components. The battery used in this vehicle model is the LiFePO4 lithium-ion battery, used in [20] and data provided by the author to integrate the battery ESS into the vehicle powertrain system model. The battery performance degradation model parameters were determined using experimental data. The model was used to determine the cost due to the battery performance degradation and shortened life. The battery is modelled after a second-order Thevenin model, which uses a resistor and capacitor combination to represent cell polarization within an open circuit voltage (OCV) framework. A figure from [20] has been used to illustrate the equivalent circuit model of the battery ESS in Figure 14.

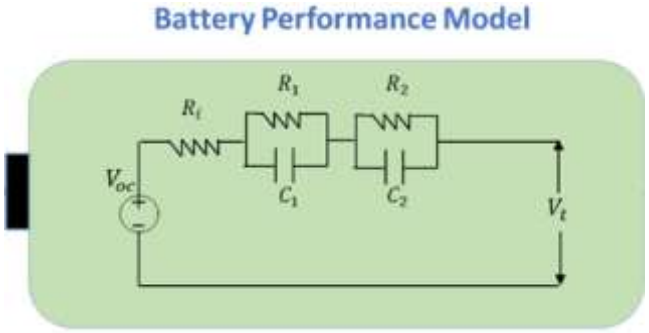

Figure 14: Battery performance model for LiFePO4 lithium ion battery [20]

Where V_{OC} is the open circuit voltage, R_i is the internal resistance, R_1/C_1 are the resistance and capacitance of the first-order cell polarization of the model, and R_2/C_2 are the resistance and capacitance of the second-order cell polarization of the model. The equations used to define the equivalent circuit model from [20] can be found below.

$$S\dot{O}C = \frac{I}{Q} \tag{3.16}$$

Where $S\dot{O}C$ is the change in battery SOC over time, I is the battery current, and Q is the battery capacity. From (3.16) a finite-difference approximation can be determined via (3.17).

$$SOC(t) = SOC(t-1) + \frac{I(t)}{Q_n}dt \tag{3.17}$$

Where $SOC(t)$ is the state of charge at a point of time t, $SOC(t-1)$ is the state of charge at the previous time step, $I(t)$ is the battery current at a point in time t, Q_n is the nominal battery capacity, and dt is the change in time in between time steps.

$$\dot{V_1} = \frac{I_{C1}}{C_1} = -\frac{V_1(t)}{R_1C_1} + \frac{I(t)}{C_1} \tag{3.18}$$

Where $\dot{V_1}$ is the change in voltage over time for the first-order cell polarization, I_{C1} is the current across the first-order cell polarization, R_1/C_1 are the resistance and capacitance of the first-order cell polarization, respectively, $V_1(t)$ is the voltage of the first-order cell polarization at a point in time t, and $I(t)$ is the current at the point in time t.

$$\dot{V_2} = \frac{I_{C2}}{C_2} = -\frac{V_2(t)}{R_2C_2} + \frac{I(t)}{C_2} \tag{3.19}$$

Where $\dot{V_2}$ is the change in voltage over time for the second-order cell polarization, I_{C2} is the current across the second-order cell polarization, R_2/C_2 are the resistance and capacitance of the second-order cell polarization, respectively, $V_2(t)$ is the voltage of the second-order cell

polarization at a point in time *t*, and $I(t)$ is the current at the time *t*.

Battery degradation was calculated via differential voltage analysis, which can be found by capturing the dV/dQ ratio of discharge profiles using different battery cycle numbers. This profile was captured through experimental data in [20] and imported into the Simulink vehicle model's ESS subsystem. There are 38 different sets of battery parameters based on degradation captured at 38 different ranges over 2000 battery cycles. For this vehicle model, the differential voltage analysis was captured by calculating values between the two degradation ranges based on the number of battery cycles that have occurred. The vehicle model in this work assumes the battery is new, and the first two ranges of battery degradation parameters are used for initializing calculations. The equations below outline how the vehicle model calculates voltage and charge at each time step, based on the differential voltage analysis.

$$V_{i,j}(t) = I(t)R_{i,j} \tag{3.20}$$

Where *i* is the index denoting the i^{th} position along the total number of time steps in the model, and *j* is the index denoting the range of degradation parameters.

$$V_{1,j}(t) = \frac{\left((1 - dt)\left(V_{1,j}(t-1)\right)\right)}{R_{1,j}C_{1,j}} + \frac{dt}{C_{1,j}I(t-1)} \tag{3.21}$$

Where $V_{1,j}(t)$ is the voltage loss from first-order cell polarization at each time step at index *j*, and $(t-1)$ denotes the previous time step.

$$V_{2,j}(t) = \frac{\left((1 - dt)\left(V_{2,j}(t-1)\right)\right)}{R_{2,j}C_{2,j}} + \frac{dt}{C_{2,j}I(t-1)} \tag{3.22}$$

Where $V_{2,j}(t)$ is the voltage loss from second-order cell polarization at each time step at index *j*.

$$V_{t,j}(t) = V_{\text{OC},j}(t) - V_{i,j}(t) - V_{1,j}(t) - V_{2,j}(t) \tag{3.23}$$

Where $V_{t,j}(t)$ is the voltage at time step *t* at index j, $V_{\text{OC},j}(t)$ is the open-circuit voltage, and $V_{i,j}(t)$ is the voltage loss due to internal resistance from the battery.

$$V(t) = \frac{cycle_{\text{real}} - cycle_{j-1}}{cycle_{j-1} - cycle_j}\left(\left(V_{t,j-1}(t) - V_{t,j}(t)\right) + V_{t,j-1}(t)\right) \tag{3.24}$$

Where $V(t)$ is the overall battery voltage at time *t*, $cycle_{\text{real}}$ represents the number of battery cycles experienced by the ESS, $cycle_j$ is the upper bound of degradation parameters, $cycle_{j-1}$

is the lower bound of degradation parameters, $V_{t,j}(t)$ is the voltage calculated from the upper bound of the degradation parameters at time *t*, and $V_{t,j-1}(t)$ is the voltage calculated from the lower bound of the degradation parameters at time *t*.

$$Q(t) = \frac{cycle_{\text{real}} - cycle_{j-1}}{cycle_{j-1} - cycle_j}\left(\left(Q_{t,j-1} - Q_{t,j}\right) + Q_{t,j-1}\right) \tag{3.25}$$

Where $Q(t)$ is the overall battery capacity at time *t*, $Q_{t,j}$ is the battery capacity calculated from the upper bound of the degradation parameters at time *t*, and $Q_{t,j-1}$ is the battery capacity calculated from the lower bound of the degradation parameters at time *t*.

As can be seen from (3.24) and (3.25), based on the number of battery cycles experienced by the vehicle model's ESS, the ESS voltage and charge are linearly interpolated based on the calculations at the upper and lower bounds of the closest established degradation parameters on either end of the actual number of battery cycles. In terms of determining how the number of battery cycles are calculated, integrating a dynamic counter of battery cycles while the model runs involve modifications to the initial work provided at [20]. The battery model at [20] required knowing how many battery cycles were going to take place beforehand, whereas that isn't feasible in a dynamic vehicle model; vehicle models calculate battery cycles while the model is running and cannot be predicted ahead. Therefore, a different approach is required. Papers from [21], [22], and [23] have solved this problem through the use of the 'Rainflow' counting algorithm. While the traditional definition of a battery cycle is a full charge and full discharge of the battery, this isn't feasible for the vehicle model, as standard energy management strategies for batteries will keep the SOC within a specific range to prevent a large depth of discharge (DOD), and as such minimize the rate of battery degradation. The Rainflow counting algorithm detects the local maxima and minima from the SOC signal. It calculates the number of cycles based on the relative amplitude size of the local maxima and minima. MATLAB has a built-in Rainflow counter function that determines the number of cycles in a signal as the model runs. Figure 15, taken from [24], illustrates the algorithm taken by MATLAB.

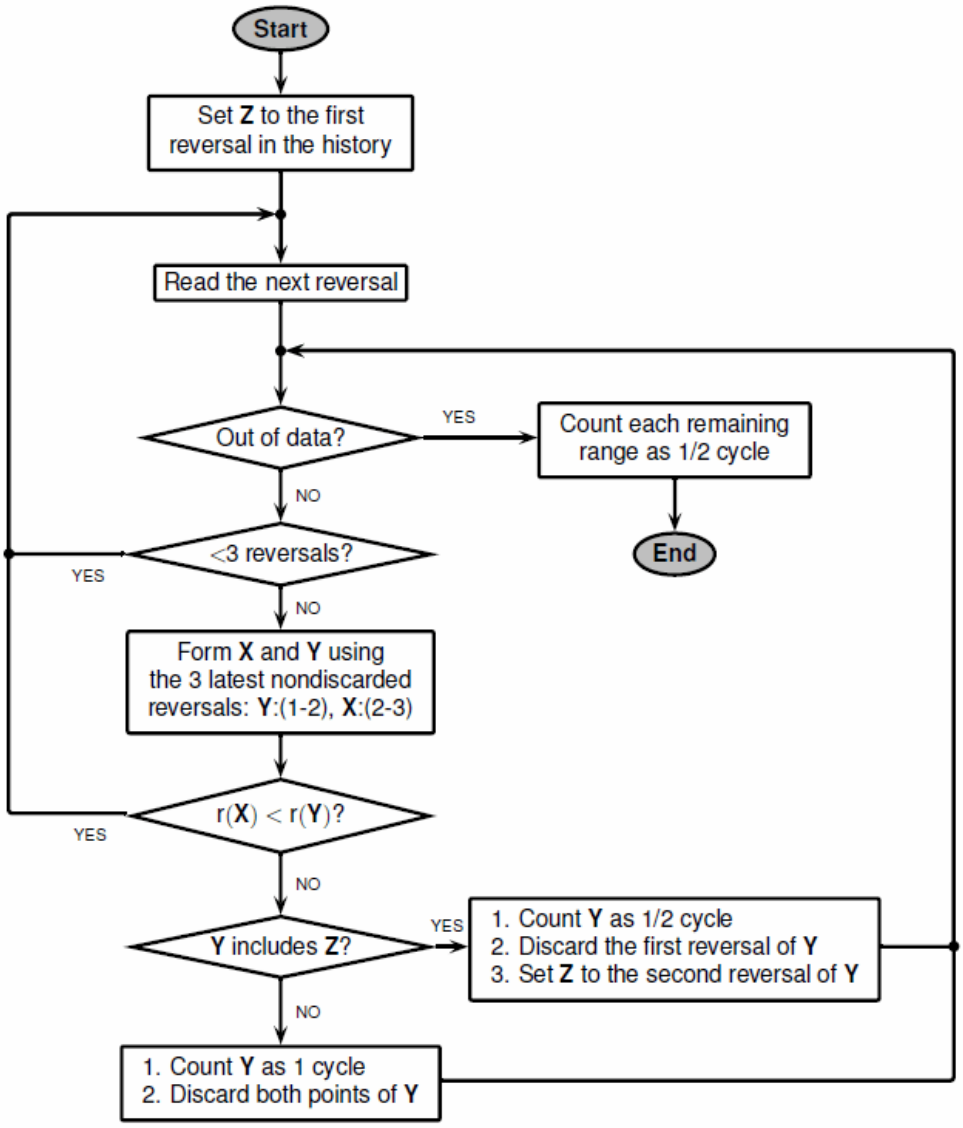

Figure 15: Rainflow counter algorithm [24]

The description from [21] is as follows:

"Reversals are the local minima and maxima where the ESS current changes sign. The function counts cycles by considering a moving reference point of the sequence, Z, and a moving ordered three-point subset with these characteristics:

a) The first and second points are collectively called **Y**.

b) The second and third points are collectively called **X**.

c) In both **X** and **Y**, the points are sorted from earlier to later in time, but are not necessarily consecutive in the reversal sequence.

d) The range of **X**, denoted by **r**(**X**), is the absolute value of the difference between the amplitude of the first point and the amplitude of the second point. The definition

of **r**(**Y**) is analogous."

Therefore, following the algorithm illustrated in Figure 15 and the above characteristics, the algorithm for the vehicle model can be summarized as follows:

a) The start point Z for the SOC signal starts at the initial SOC state of the ESS. For the purposes of this model, the initial state of the SOC starts at 99%.
b) The ESS battery discharges until it either receives a charge from regenerative braking or from the energy management controller maintaining the target ESS value of 60% SOC. The valley where SOC stops discharging and switches to charging forms the second reversal.
c) The point in time in the model where the SOC stops charging and starts discharging forms a third reversal, which then enables an evaluation from the algorithm.
d) The range of X is compared against the range of Y. If the range of X is smaller, then the algorithm expands its search to the next reversal. If the range of X is greater than the range of Y, then the algorithm moves forward to determine whether the battery cycles counts as a full cycle, or a half cycle.
e) If point Z is one of the reversals within the range of Y, a 'half battery cycle' is added to the total cycle count; the first reversal in Y gets discarded, and then point Z moves on to the next reversal. The algorithm then loops back to check for more reversals.
f) If point Z is not one of the reversals within the range of Y, then a full cycle is added to the cycle count. Both reversals in the range of Y are dropped, and the algorithm then loops back to check for more reversals.
g) When no reversals remain to be evaluated, all remaining ranges are counted as a half cycle, and the algorithm ends.

As the cycles pass the thresholds defined by the degradation parameters, Stateflow updates the degradation parameters for both j and (j -1) as used in (3.20) through (3.25), thus dynamically updating the ESS calculations while the model runs.

3.3. Vehicle Operation Simulations Using the Model

Once the operation profile has been established and the vehicle model has been built, the next step is to run the model to obtain simulation results. The FCEV model is compared to an equivalent ICEV model as a benchmark to determine the feasibility of the vehicle model design.

3.3.1 Definition of a Viable Design Solution

A viable vehicle design solution is identified by adjusting the vehicle powertrain design and controls to arrive at a design with the minimum fuel consumption and powertrain component degradation costs. An additional constraint is that the viable solution must also meet the operational range requirements of the armoured vehicle, as the scenario modelled is not the only one the armoured vehicle would be required to do in a real-life setting. Given that the vehicle model is an approximation of the TAPV, from [17] the operational range of a TAPV is defined as 654 km. Therefore, all viable solution candidates will have their operation profile looped until the vehicle model covers, at minimum, the operational range. The control is designed to cut off if the ESS SOC is equal to or less than 1%. If the vehicle runs out of fuel, the viable solution candidate will be discarded if the vehicle model fails to meet the operational range requirement.

3.3.2 ESS Configurations

A total of 40 ESS configurations were evaluated for the vehicle model: between 1 and 8 battery packs in series, and 1 and 5 battery packs in parallel. A battery pack is defined as 20 battery cells connected in series, which was determined arbitrarily for not having to evaluate the model over every single battery cell increment. As a larger vehicle, such a focus would not be an efficient use of computation time, as it would both be expensive and not yield meaningful results between smaller, individual batteries. Determining an upper limit for battery pack size was challenging because, typically, vehicle dimensions and organizational budgets put both physical and financial constraints on design, where this vehicle model has no real-world metrics to work with. One cannot also simply take TAPV internal dimensions and use those, as one cannot simply replace one-for-one the ICEV powertrain configuration with the FCEV one. A complete redesign of the interior would be required, which requires moving many hard-to-install wires, cryptographic equipment, and space to carry soldiers as well as their weapons and gear. Therefore, an upper limit of 8 battery packs in series and 5 battery packs in parallel (800 battery cells in total) was determined to arbitrarily serve as the upper limit of ESS size, with the idea that if no feasible solutions were found within the ESS range provided to the vehicle model, that the search parameters would then be expanded.

3.4. Post-Processing

The models were implemented in MathWorks' MATLAB/Simulink. The MATLAB script loops through running the model under different ESS configurations, recording the total fuel consumed during the trip, as well as the total cost due to degradation losses from both the fuel cell systems and the ESS packs, writing these results into the MATLAB workspace as arrays. From these arrays, the total cost of each trip was calculated.

3.4.1 Fuel Cell Degradation Equations

Equation (2.1) was used to calculate the degradation cost of the fuel cell systems of the vehicle model as the operation profile was evaluated. The one challenge experienced in making a feasible equation was that capital costs also needed to be factored into the viable solution. For example, having a larger fuel cell system and ESS configuration will have a smaller depth of discharge, which will lead to lower operating costs; however, it is misleading to think that is the cheapest solution, as the upfront costs of acquiring larger powertrain components is more expensive. Therefore, in order to better capture the capital cost of the powertrain as a function of the operation profile, the powertrain component's RUL is taken into account.

$$RUL_{\text{Fuel Cell}} = 1 - \frac{\left(\xi_{\text{low}} t_{\text{low}} + \xi_{\text{high}} t_{\text{high}} + \xi_{\text{chg}} \eta\right)}{\Delta V} \tag{3.26}$$

Where $RUL_{\text{Fuel Cell}}$ is the remaining useful life of the fuel cells, ΔV is the maximum allowable voltage degradation of the fuel cell system, ξ_{low} and t_{low} represents the degradation value and time when the fuel cell is idling (defined as being turned on and up to 10% of the fuel cell systems' maximum power), ξ_{high} and t_{high} represent degradation value and time spent under high power load (defined as using 90% of the fuel cell systems' maximum power), ξ_{chg} represents the degradation value of a dynamic load (defined as when the fuel cell systems switch from idle to its rated power), and η represents the number of times the fuel cell systems are subjected to a changing load. The following logic is used to shape (3.26) into another equation used for costing:

The study from [8] defined the maximum allowable voltage degradation of the fuel cell systems to be a maximum of 10% from the initial factory value.

$$Degradation_{\text{Fuel Cell Stack}} = \left(\xi_{\text{low}} t_{\text{low}} + \xi_{\text{high}} t_{\text{high}} + \xi_{\text{chg}} \eta\right) M \tag{3.27}$$

Where M is the total number of fuel cells in the fuel cell system.

After the vehicle model has finished evaluating the operation profile, assuming a linear rate of degradation, the maximum number of times the operation profile can be driven before the fuel cell systems require replacement are noted in (3.28).

$$Max\ \#\ of\ trips_{\text{Fuel Cell}} = \frac{Degradation_{\text{Fuel Cell Stack}}}{0.1} \tag{3.28}$$

Once the maximum number of trips of the operational profile has been determined, a capital cost associated with the degradation of the fuel cell systems may finally be applied to the operation profile.

$$Degradation\ Cost\ Per\ Trip_{\text{Fuel Cell Stack}} = \frac{C_{\text{FC}}\ P_{\text{nom}}}{Max\ \#\ of\ trips} \tag{3.29}$$

Where C_{FC} is the PEMFC manufacturing cost per unit power, and P_{nom} is the nominal power from the fuel cell system. Degradation in cost per trip is used as part of the final calculation for the costs associated with evaluating the vehicle's performance when subjected to the operation profile.

3.4.2 Battery Degradation Model

The methodology of calculating battery degradation is similar to the process outlined in 3.4.1. The papers from both [8] and [12] use a value of 20% battery degradation before requiring replacement, therefore that value will be used in this work when determining RUL. The equations below outline the process of calculating the capital costs associated with ESS degradation. The battery capacity from the vehicle model is calculated from (3.5), and the maximum allowable battery capacity is calculated from (2.2). From these, equations to determine ESS cost can be built.

$$Degradation_{\text{ESS}} = Ah_{\text{cycle}} \tag{3.30}$$

Where Ah_{cycle} is the battery capacity after the operation profile is evaluated, calculated from Eq. (3.5).

$$Max\ \#\ of\ trips_{\text{ESS}} = \frac{Degradation_{\text{ESS}}}{0.2} \tag{3.31}$$

$$Degradation\ Cost\ Per\ Trip_{\text{ESS}} = \frac{C_{\text{batt}} E_{\text{nom}}}{Max\ \#\ of\ trips} \tag{3.32}$$

Where C_{batt} is the cost of the battery per unit power, and E_{nom} is the battery nominal energy capacity.

3.5. Benchmark ICEV

To serve as a comparison against the FCEV, a benchmark ICEV model was created as an approximation of the TAPV, using the same chassis and wheel parameters as the FCEV model. The vehicle uses a forward-looking model, similar to the FCEV, to predict the speed and match the desired speed trace. The accelerator/brake pedal sends a signal to the combustion engine, where torque is transferred in sequence to the clutch, transmission, torque converter, final drive, and then lastly, the wheels, which propel the vehicle chassis forward. The table below highlights the key parameters for the benchmark ICEV.

Table 9: Key parameters for benchmark vehicle

Parameter Name	Value (Units)
Vehicle Mass	18000 (kg)
Chassis Drag Coefficient	0.7
Chassis Frontal Area	7.12 (m^2)
ChassisRatio of Weight in the Front	0.4
Chassis Length	6.31 (m)
Chassis Width	2.75 (m)
Chassis Height (with wheels)	3.225 (m)
Wheel Aspect Ratio	90
Wheel Radius	0.6604 (m)
Wheel Coefficient of friction	0.7
Number of Gears	4
Gear Ratio #1	3.0270
Gear Ratio #2	1.6194
Gear Ratio #3	1.0000
Gear Ratio #4	0.9644
Engine Max Power	350000 kW
Final Drive Ratio	15.0000
Torque Coupling Ratio	0.4500

One of the most significant differences between the ICEV and FCEV, apart from their different powertrain configurations, is the lack of a vehicle controller in the ICEV for the energy management system. The ICEV's lead-acid battery is used to start the vehicle and is not of the vehicle propulsion system; therefore, there is no requirement to regulate power demand between the fuel converter and the ESS for efficiency purposes. This resulted in a faster vehicle model simulation and was easier overall to match demanded speed versus actual vehicle speed.

Chapter 4. Results from Evaluating the Vehicle Model

The vehicle model was run and evaluated using the operation profile under different ESS configurations. The total trip cost of the operation profile, based on ESS configuration, was captured and the cost of fuel consumed. Fuel consumption was compared against the benchmark ICEV for comparison.

4.1. Cost of Fuel Consumption

4.1.1 Cost of Fuel Consumption for the FCEV

The amount of hydrogen fuel consumed and associated costs for the FCEV vehicle model using the operation profile with different ESS configurations as outlined below.

Table 10: Hydrogen fuel consumed from operation profile based on ESS configuration

Amount of Hydrogen Fuel Consumption (L)

	1x ESS packs in parallel	2x ESS packs in parallel	3x ESS packs in parallel	4x ESS packs in parallel	5x ESS packs in parallel
1x ESS packs in series	0.3350	1.0019	0.9378	0.5126	0.0525
2x ESS packs in series	1.2411	0.2383	0.0518	0.0508	0.0508
3x ESS packs in series	0.2749	0.0517	0.0508	0.0508	0.0508
4x ESS packs in series	0.1495	0.0508	0.0508	0.0508	0.0508
5x ESS packs in series	0.0520	0	0	0	0
6x ESS packs in series	0.0517	0	0	0	0
7x ESS packs in series	0.0508	0	0	0	0
8x ESS packs in series	0	0	0	0	0

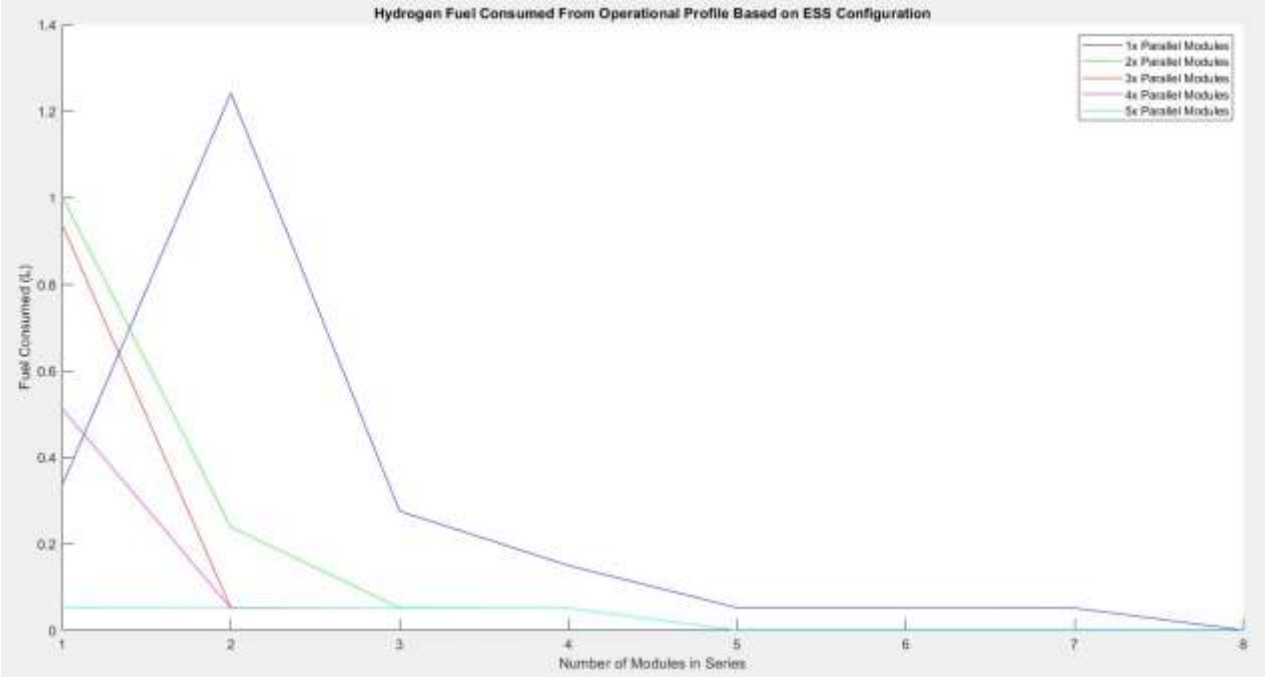

Figure 16: Cost of consumed hydrogen fuel from operation profile for ESS configuration

Table 11: Cost of consumed hydrogen fuel from operation profile for ESS configuration

Cost of Hydrogen Fuel Consumption ($)

	1x ESS packs in parallel	2x ESS packs in parallel	3x ESS packs in parallel	4x ESS packs in parallel	5x ESS packs in parallel
1x ESS packs in series	7.0544	21.0998	19.7495	10.7950	1.1065
2x ESS packs in series	26.1373	5.0183	1.0901	1.0704	1.0704
3x ESS packs in series	5.7901	1.0897	1.0702	1.0702	1.0702
4x ESS packs in series	3.1477	1.0699	1.0699	1.0699	1.0699
5x ESS packs in series	1.0941	0	0	0	0
6x ESS packs in series	1.0893	0	0	0	0
7x ESS packs in series	1.0698	0	0	0	0
8x ESS packs in series	0	0	0	0	0

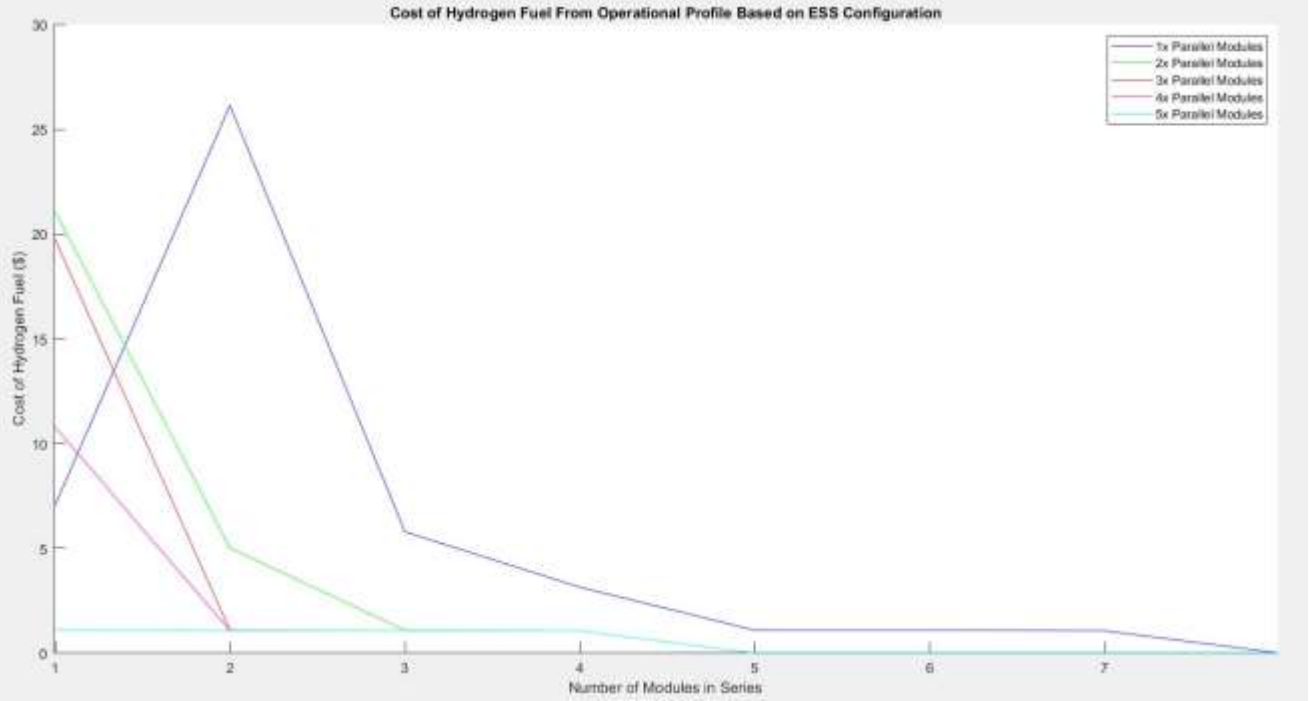

Figure 17: Cost of hydrogen fuel from operation profile based on ESS configuration

As can be seen from Figures 16 and 17, with the exception of a single data point on the graph, as the ESS battery pack for the vehicle model grows in size, the cost and consumption of hydrogen fuel decreases. This trend is to be expected, as the larger the size of the ESS, the more it is able to expend its charge to meet the vehicle's power demand without the use of the hydrogen fuel cell system. These results will be further covered in the Discussion section of the paper.

The benchmark vehicle used a total of 0.9288 litres of diesel fuel, using the average price of diesel per litre from [25] of $1.267, which given the low and unchanging speeds of the operation profile, is not an unreasonable value in terms of fuel consumption. The total cost of fuel from the benchmark vehicle is $1.177 for the operational trip.

4.2. Total Trip Cost of the Operation profile

Factoring in the capital costs and degradation of the fuel cell system and ESS powertrain components, the total trip cost based on ESS configuration is outlined below, including separate tables highlighting individual costs for the fuel cell systems and ESS configurations.

Table 12: Cost of fuel cell degradation from operation profile

Cost of Fuel Cell Degradation from Operation profile ($)

	1x ESS packs in parallel	2x ESS packs in parallel	3x ESS packs in parallel	4x ESS packs in parallel	5x ESS packs in parallel
1x ESS packs in series	0.0051	0.0050	0.0045	0.0048	0.0051
2x ESS packs in series	0.0043	0.0050	0.0051	0.0051	0.0051
3x ESS packs in series	0.0048	0.0051	0.0051	0.0051	0.0051
4x ESS packs in series	0.0051	0.0051	0.0051	0.0051	0.0051
5x ESS packs in series	0.0051	0.0022	0.0022	0.0022	0.0022
6x ESS packs in series	0.0051	0.0022	0.0022	0.0022	0.0022
7x ESS packs in series	0.0051	0.0022	0.0022	0.0022	0.0022
8x ESS packs in series	0.0022	0.0022	0.0022	0.0022	0.0022

Table 13: Cost of ESS degradation from operation profile

Cost of ESS Degradation from Operation profile ($)

	1x ESS packs in parallel	2x ESS packs in parallel	3x ESS packs in parallel	4x ESS packs in parallel	5x ESS packs in parallel
1x ESS packs in series	99.9365	68.7466	80.7967	57.3156	42.5633
2x ESS packs in series	266.9616	218.0418	41.3261	41.1709	42.5557
3x ESS packs in series	258.0766	41.4922	41.8186	43.8409	45.4347
4x ESS packs in series	91.3088	41.1709	43.7656	45.9175	47.6929
5x ESS packs in series	42.4329	42.5957	45.4799	47.6730	49.4635
6x ESS packs in series	41.3638	43.8415	46.8131	49.0863	50.955
7x ESS packs in series	40.5172	44.8861	48.0337	58.9601	52.3277
8x ESS packs in series	41.1909	45.9175	442.7367	277.9736	18,588

Table 14: Total trip cost from operation profile based on ESS configuration

Total Trip Cost of Operation profile ($)

	1x ESS packs in parallel	2x ESS packs in parallel	3x ESS packs in parallel	4x ESS packs in parallel	5x ESS packs in parallel
1x ESS packs in series	106.9960	89.8513	100.5507	68.1154	43.6750
2x ESS packs in series	293.1033	223.0652	42.4213	42.2465	43.6313
3x ESS packs in series	263.8715	42.5870	42.8938	44.9162	46.5100
4x ESS packs in series	94.4615	42.2459	44.8406	46.9925	48.7679
5x ESS packs in series	43.5321	42.5980	45.4822	47.6752	49.4658
6x ESS packs in series	42.4583	43.8438	46.8153	49.0886	50.9977
7x ESS packs in series	41.5921	44.8883	48.0360	58.9624	52.3299
8x ESS packs in series	41.1931	45.9197	442.7389	277.9758	18,588

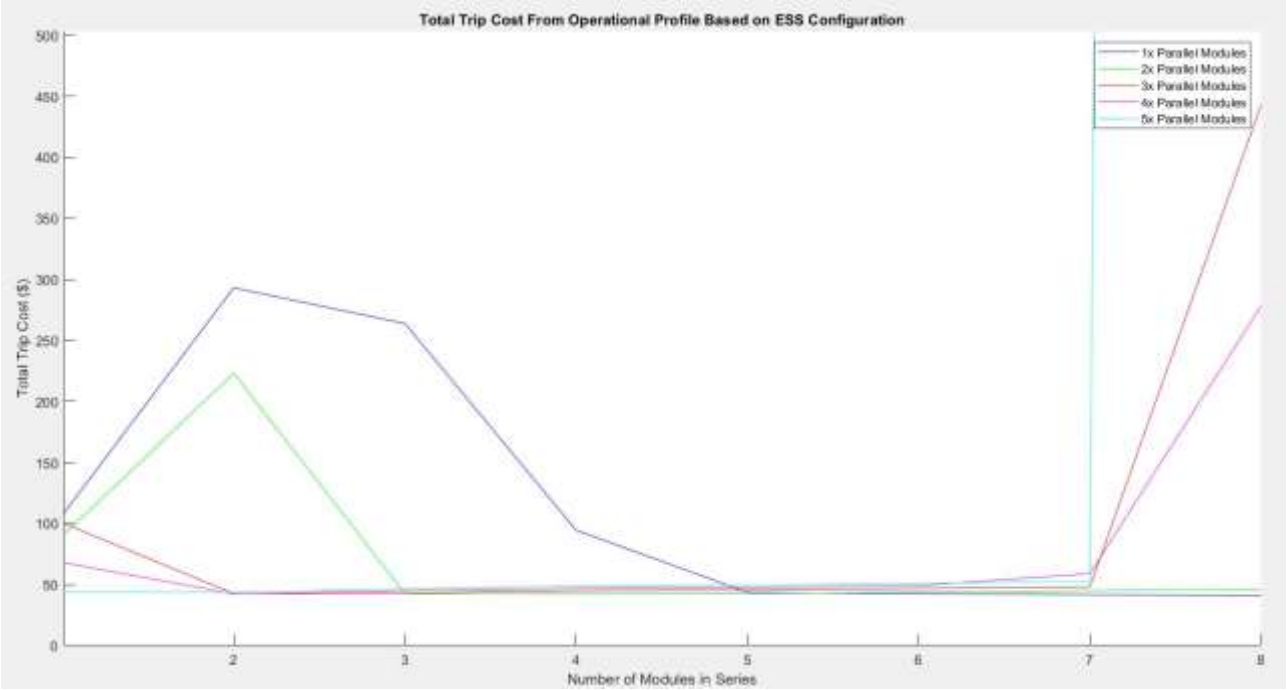

Figure 18: Total trip cost from operation profile based on ESS configuration

4.3. ESS SOC Results

Given that the energy management control strategy plays a large part in operation profile costing for the FCEV, a sample set of ESS SOCs have been plotted to help provide context to the costs in Table 14 for the Discussion section, including a figure of the gradient profile that drives the controller response.

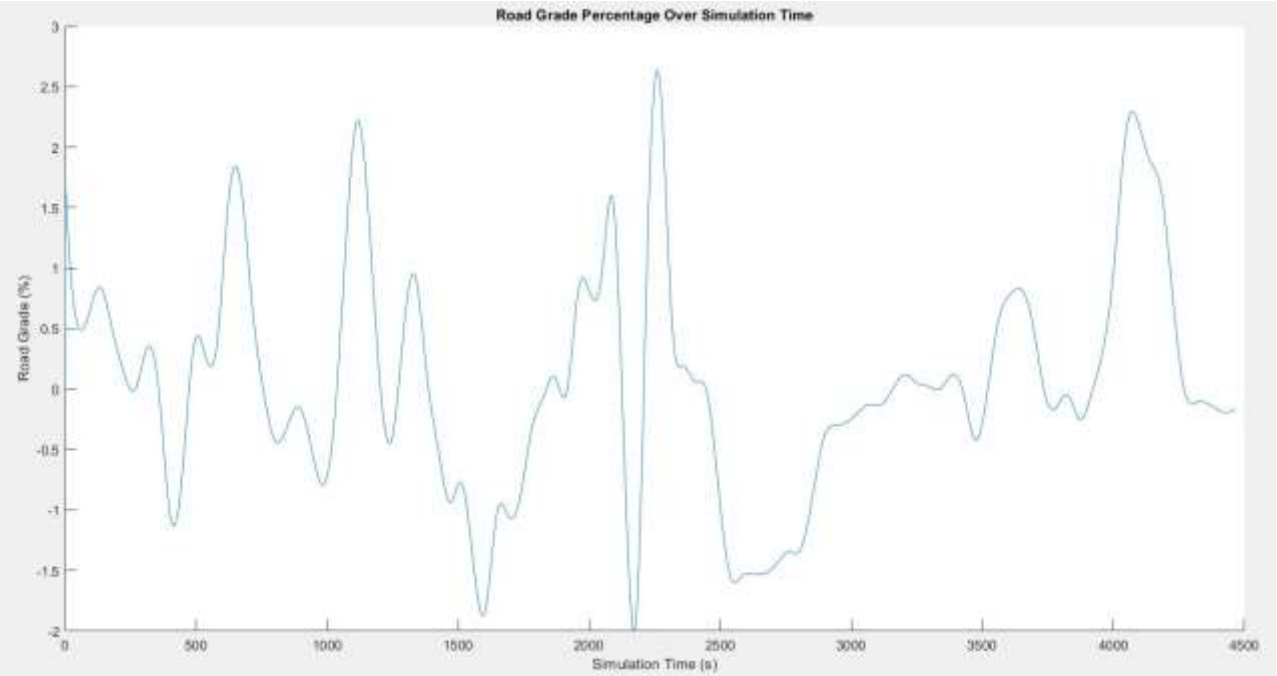

Figure 19: Road grade percentage over simulation time

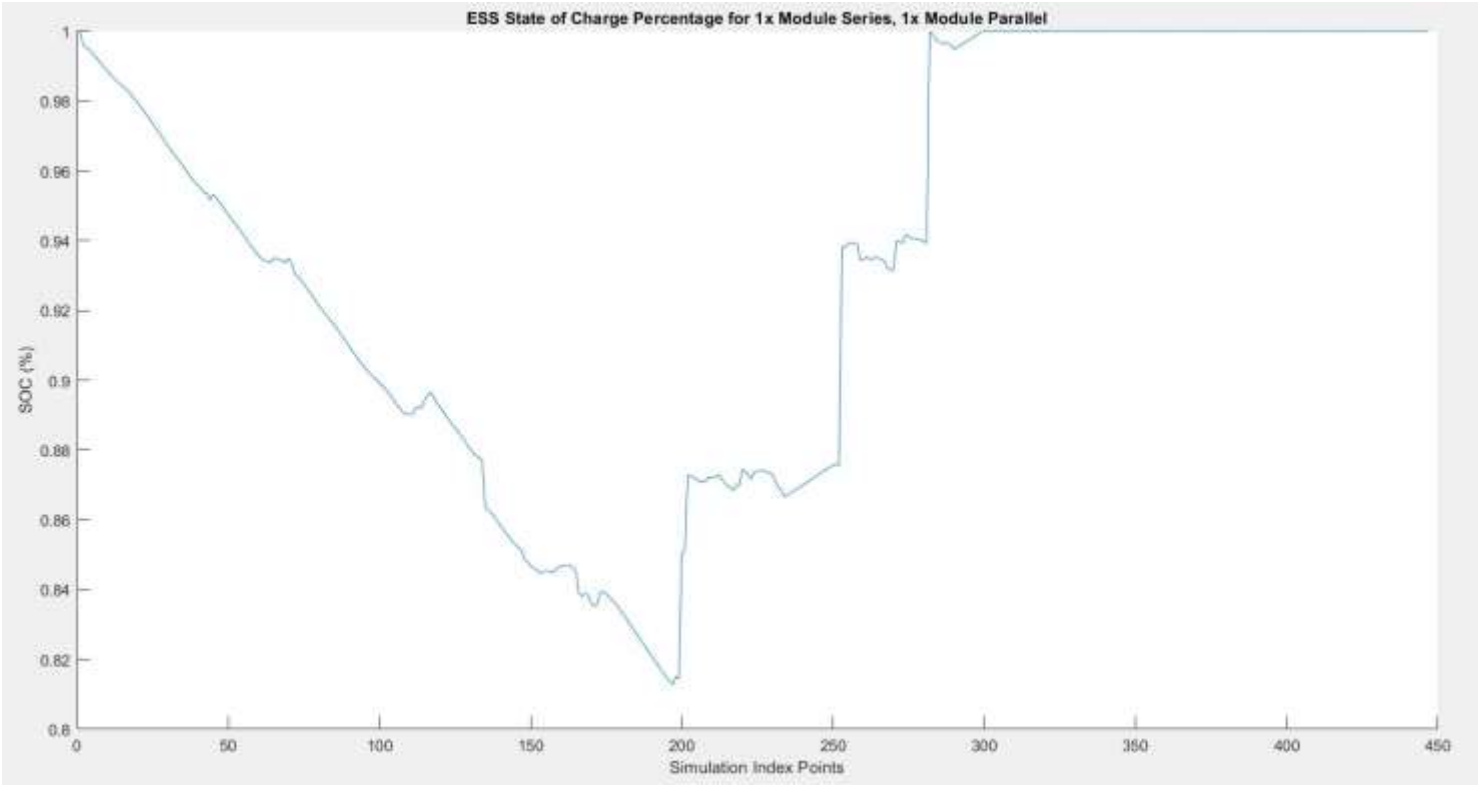

Figure 20: ESS state of charge percentage change for 1x module series, 1x module parallel

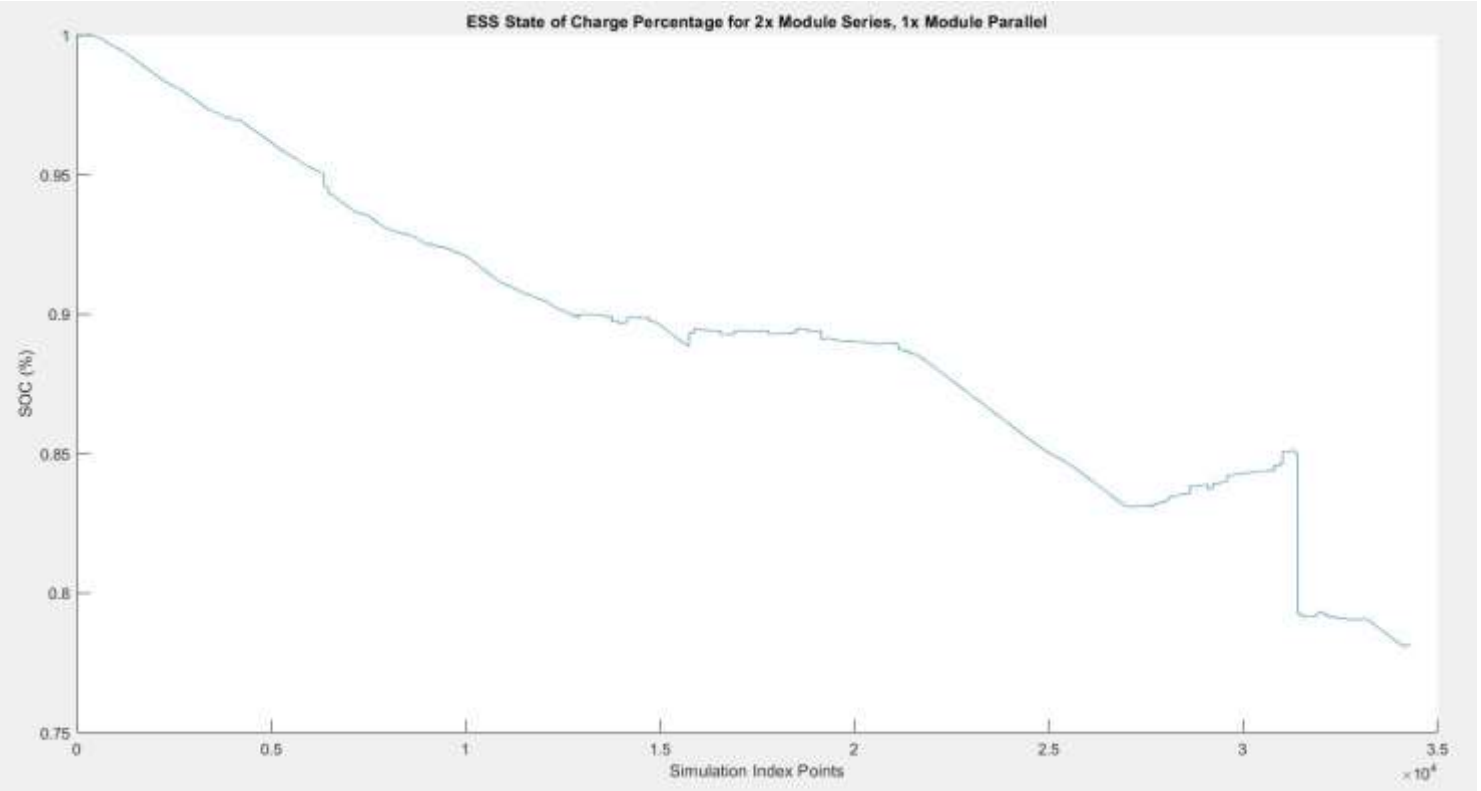

Figure 21: ESS state of charge percentage change for 2x module series, 1x module parallel

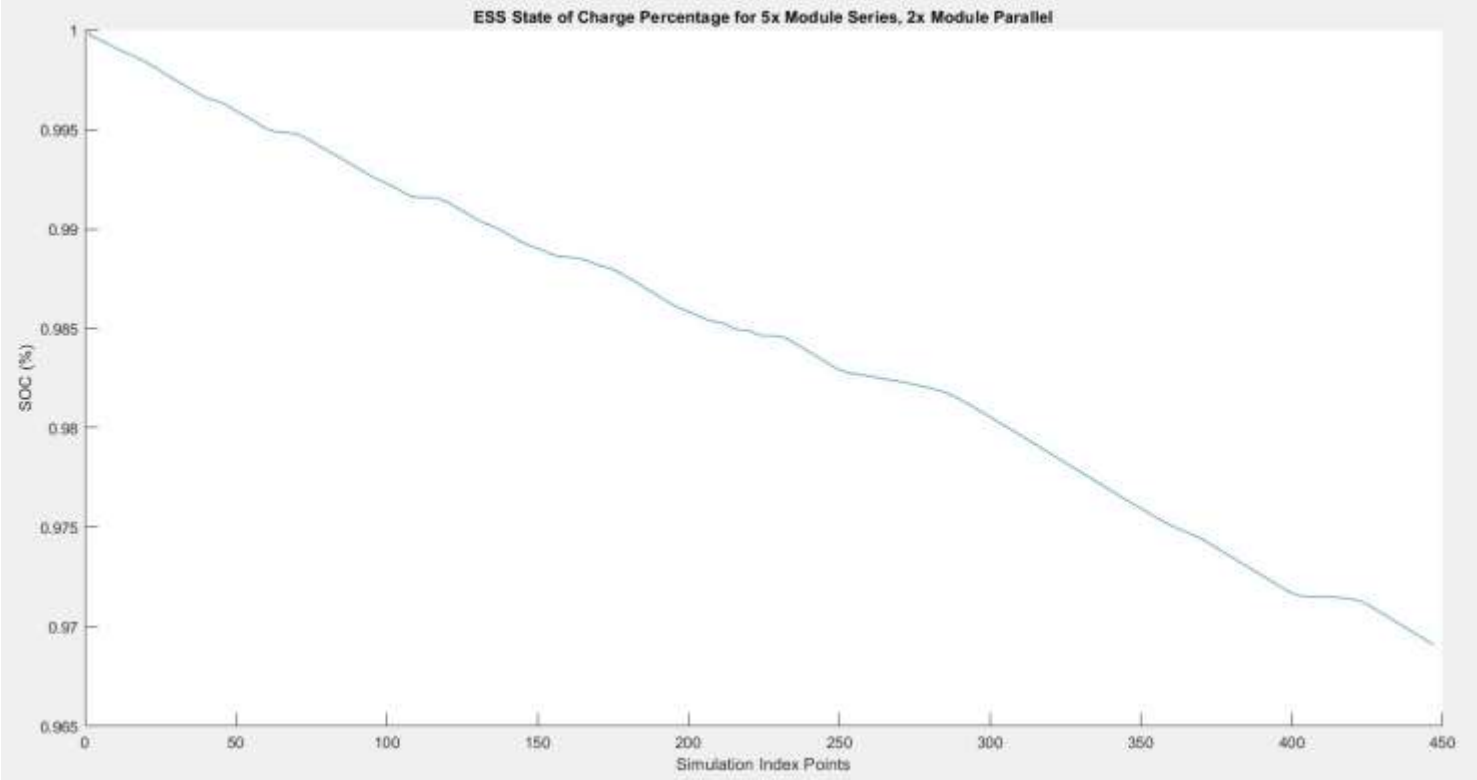

Figure 22: ESS state of charge percentage change for 5x module series, 2x module parallel

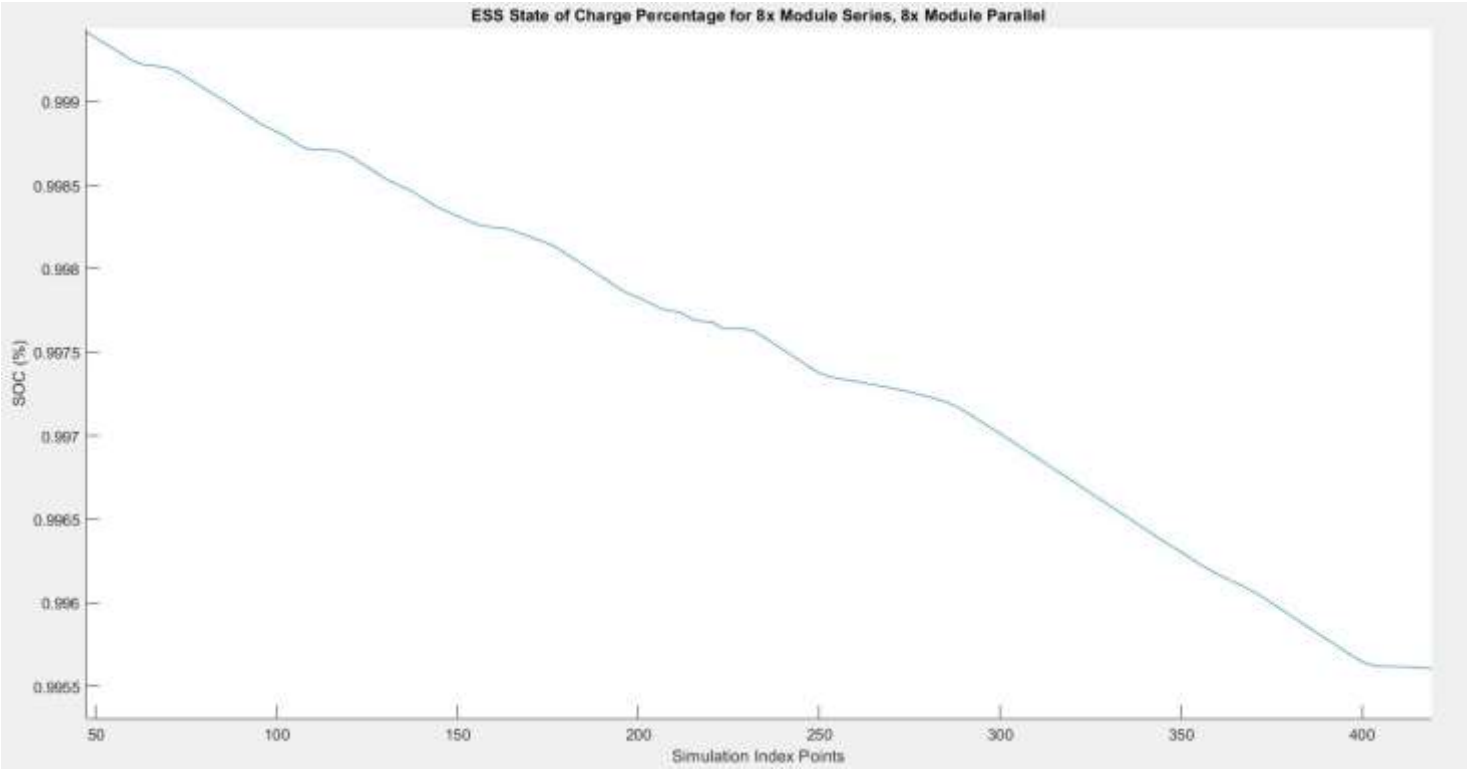

Figure 23: ESS state of charge percentage change for 8x module series, 8x module parallel

To provide additional context to the results from Table 14, some additional points are highlighted. First, this study has considered both the power and energy capabilities of the battery ESS, which get factored into the energy management strategy, influencing the overall cost of the vehicle in the operation profile. The battery configuration, measured by the number of battery cells used in the battery packs (20 battery cells per battery pack, as noted in Section 3.3.2), reflects the energy capability of the energy storage system. 100 km is a reasonable range for routine military tasks, and therefore to minimize the usage of the more expensive PEMFC system and associated hydrogen fuel, the lower bound of 18 Ah battery capacity and 60 V nominal voltage (assuming ideal values prior to dynamic degradation) was used to provide the appropriate power to satisfy the power demand of the operation profile. Similarly, due to cost constraints of a budget and size constraints of the physical vehicle, the upper bound of 144 Ah battery capacity and 480 V (assuming ideal values before dynamic degradation) was selected for the battery configuration. Through seeking to minimize the cost of the operation profile through fuel consumption and powertrain component degradation, this work sought out the ideal battery ESS configuration that provided the minimum cost, while also meeting the vehicle's performance requirements. This is in addition to ensuring all battery ESS configurations can work in parallel with the PEMFC to ensure the minimum power needs to provide the demanded vehicle propulsion are also met.

4.4. Operational Range Verification and Optimal Solution

To be considered a feasible solution, the vehicle model must be capable of driving up to the operational range of the vehicle. From [17], the operational range of the TAPV is 654 km, so with an operation profile trip distance of 18.589 km, a scaling factor can be applied to the hydrogen consumed each trip to determine if it exceeds the vehicle's hydrogen tank capacity of 35 kg. This work uses a SOC of 100%, operating at other initial conditions for SOC is out of scope and may be considered under future work.

$$Scaling\ Factor = \frac{Operational\ Range}{Operational\ Profile\ Distance} \tag{4.1}$$

$$Scaling\ Factor = \frac{654\ km}{18.589\ km} = 35.182 \tag{4.2}$$

Applying (4.2) to Table 10, a new table can be created to show if a solution may be considered feasible (F) or not feasible (NF).

Table 15: Feasibility of vehicle model solutions based on operational range

Hydrogen Consumed over the Vehicle's Operational Range (kg)

	1x ESS packs in parallel	2x ESS packs in parallel	3x ESS packs in parallel	4x ESS packs in parallel	5x ESS packs in parallel
1x ESS packs in series	11.786 (F)	35.249 (NF)	32.994 (F)	18.034 (F)	1.847 (F)
2x ESS packs in series	43.664 (NF)	8.384 (F)	1.822 (F)	1.787 (F)	1.787 (F)
3x ESS packs in series	9.672 (F)	1.819 (F)	1.787 (F)	1.787 (F)	1.787 (F)
4x ESS packs in series	5.260 (F)	1.787 (F)	1.787 (F)	1.787 (F)	1.787 (F)
5x ESS packs in series	1.829 (F)	0 (F)	0 (F)	0 (F)	0 (F)
6x ESS packs in series	1.819 (F)	0 (F)	0 (F)	0 (F)	0 (F)
7x ESS packs in series	1.787 (F)	0 (F)	0 (F)	0 (F)	0 (F)
8x ESS packs in series	0 (F)	0 (F)	0 (F)	0 (F)	0 (F)

As can be seen in Table 15, only two ESS configurations are not feasible solutions based on the operational range as a constraint: the ESS with 2x module packs in series and 1x module pack in parallel, and the ESS with 2x module packs in series and 2x module packs in parallel. The optimal solution can be further refined by finding the minimal cost of the operation profile trip, which was the ESS configuration with 8x modules in series and 1x module in parallel, with a total operation profile cost of 41.1931.

4.5. Vehicle Speed Signal Validation

4.5.1 Root Mean Square Error

The results include ensuring that the signal representing the simulated vehicle speed matches the demanded vehicle speed as closely as possible. One of the two methods selected to evaluate this was to calculate the root mean square error (RMSE) between the two signals using the equation below.

$$RMSE = \sqrt{\sum_{n=1}^{N} \frac{(\hat{y}_i - y_i)^2}{N}} \tag{4.2}$$

Where n is the index in a sum of N total waypoints, $\hat{y}_i$ is the predicted value (demanded vehicle speed), and y_i is the actual value (actual vehicle speed). Applying (4.2) to the different ESS configurations, their corresponding RMSE values get populated in the table below.

Table 16: RMSE values based on ESS configuration for operation profile

RMSE Values Based on ESS Configuration for Operation profile

	1x ESS packs in parallel	2x ESS packs in parallel	3x ESS packs in parallel	4x ESS packs in parallel	5x ESS packs in parallel
1x ESS packs in series	0.0389	0.0347	0.0353	0.0355	0.0268
2x ESS packs in series	0.0302	0.0489	0.0251	0.0236	0.0236
3x ESS packs in series	0.0840	0.0252	0.0236	0.0236	0.0236
4x ESS packs in series	0.2953	0.0236	0.0236	0.0236	0.0236
5x ESS packs in series	0.0267	0.0236	0.0236	0.0236	0.0236
6x ESS packs in series	0.0251	0.0236	0.0236	0.0235	0.0236
7x ESS packs in series	0.0235	0.0236	0.0235	0.0235	0.0236
8x ESS packs in series	0.0236	0.0236	0.0236	0.0236	0.0236

For the benchmark vehicle, there was only one configuration, with an RMSE value of 0.0093. The mean value of RMSE for all ESS configurations is 0.0342.

4.5.2 Maximum Absolute Error

While RMSE values help depict an overall picture of error when comparing two datasets, maximum absolute error (MAE) gives the value of the data point in the set that deviates most from the signal it is being compared against. In the case of the vehicle model, the MAE values represent the waypoint where the actual vehicle speed deviates the most from the demanded

vehicle speed value, which serves as an indicator of the lowest point in the vehicle controller's performance.

Table 17: MAE values based on ESS configuration for operation profile

MAE Values Based on ESS Configuration for Operation profile

ESS packs in series	Number of ESS packs in parallel				
	1	2	3	4	5
1x ESS packs in series	1.2159	0.8583	0.7550	0.7039	0.4947
2x ESS packs in series	0.3926	0.6912	0.3715	0.1302	0.1343
3x ESS packs in series	2.0608	0.3724	0.1317	0.1344	0.1349
4x ESS packs in series	7.3905	0.1302	0.1289	0.1358	0.1325
5x ESS packs in series	0.4895	0.1290	0.1324	0.1353	0.1345
6x ESS packs in series	0.3658	0.1344	0.1316	0.1334	0.1283
7x ESS packs in series	0.1269	0.1266	0.1075	0.1157	0.1235
8x ESS packs in series	0.1168	0.1196	0.1172	0.1201	0.1201

For the benchmark vehicle, there was an MAE value of 0.4855. The mean value for MAE across all ESS configurations was 0.4902.

Chapter 5. Discussion

There are two important topics that need to be reviewed in the discussion of this work: the interpretation of the results and reviewing potential sources of error. The latter is particularly important to cover, given the challenges in validating this relatively novel vehicle model.

5.1. Interpretation of Results

5.1.1 Cost Trends

Hydrogen Fuel Consumed

Based on Table 11, the most expensive hydrogen fuel consumption comes not from the smallest ESS configuration, but rather from one ESS pack in series with multiple modules in parallel, and one module in parallel with multiple modules in series. Figures 20 and 21 are compared side-by-side. Figure 20 shows a sharp drop in discharge, followed by a rapid charging of the ESS before maintaining a constant charge near 100% SOC for the remainder of the simulation. This suggests the vehicle controller uses the HEV charge saturation (Figure 8 refers) mode for the second half of the simulation, meaning the power demand for the ESS is less than the max regen for the ESS that the fuel cell system can support. Given that this is the smallest ESS configuration tested, this behaviour appears to be logical. Compared to the gradient profile, the battery cannot meet the power demand for the gradient climb around the 2200 second mark, where the fuel cell system then picks up the power demand for both propelling the vehicle and charging the ESS. As for Figure 21, instead of a deep discharge followed by a rapid charging, the SOC plateaus around the area where the most significant climb in road gradient is. This suggests that the controller is straddling the line between regular HEV operation where the ESS power demand is such that the system is charging and discharging the ESS, which involves supporting the fuel cell system. Though the SOC required more charging in Figure 20 than Figure 21, the ESS configuration in Figure 21 is twice as large, meaning the fuel cell system has to work harder to charge the larger battery, thus consuming more fuel overall, resulting in a more expensive operation profile trip fuel-wise. It was not until the ESS configuration was 5 modules in series and 2 modules in parallel that the cost of hydrogen fuel became zero, meaning the ESS satisfied the vehicle's power demand for the entire duration of the operation profile trip.

Figure 22 showed that no support from the fuel cell systems is provided to the ESS, only

regenerative braking from the corresponding negative road gradient from Figure 19. The largest ESS configuration, 8 modules in series and 8 modules in parallel, has a similar SOC pattern in Figure 23 when compared to Figure 22, with the most noticeable difference being a much smaller depth of discharge due to having a much larger battery capacity to draw from.

Fuel Cell Degradation

Of the costs associated with the operation profile, degradation of the fuel cell system is by far the cheapest of the associated costs, with all operation profile trips costing less than one cent per trip. Given that the operation profile involves maintaining a steady low speed, this is not surprising given that the equation for fuel cell degradation involves transitions between loads and when under heavy load. Given that these actions were kept to a minimum, degradation due to idling was the largest source of voltage loss. In another operation profile setting where the distance is longer and/or the terrain is more challenging, it would be expected to see an increase in fuel cell degradation. Another point to note is that the vehicle model's energy management strategy prioritizes the use of the ESS over that of the fuel cell system, which further reduces its use and, by extension, its rate of degradation. It's only when the vehicle's power demand exceeds that which the ESS can provide that the fuel cells get engaged, and even when the fuel cells are engaged, it's only to the point to cover the difference that the ESS is unable to provide. Once the ESS is capable of meeting the power demand of the vehicle model again, the fuel cell system turns off until needed again.

ESS Degradation

By contrast to the fuel cells, the ESS battery packs are the most expensive aspect of the operation profile costing, which was to be expected, given the costly nature of replacing rechargeable batteries for vehicles. The most expensive battery configurations are the larger ones. Some of the larger ESS configurations have abnormally high operation profile costs, namely the ESS configurations with 8x modules in series and 3-5x modules in parallel with costs ranging from $277.98 to $18,588. Given that the vehicle is travelling approximately 18 km at a constant low speed, it is unlikely that the ESS would degrade at such an expensive rate per trip. Those three numbers are less likely due to the operation profile itself, but instead how the degradation equation is defined that factors the capital costs into the equation. While sources of model error will be covered in a future section, with such significant capital costs for larger ESS configurations, any change in the degradation values for the ESS serves as a sensitivity that results in a sizeable overall cost to the operation profile. As an example, using the $18,588 price tag for the 8x modules in series and 8x modules in parallel, given a capital

cost of $6,912,000, that amount is 0.2689% of the overall capital costs (which is noted to still be high). It is possible that once a certain battery number threshold has been passed that factoring capital costs into the equation starts to become less effective when using a linear model to represent it.

5.2. Military Takeaways from Results

ESS Configuration Size

At first glance of the results, it may be appealing to suggest that given the expensive nature of acquiring and replacing rechargeable batteries that the best solution is to instead provide the smallest possible battery that can support the fuel cell system, and let the fuel cell system provide the majority of power to the vehicle. However, it is worth noting that the military values redundancies in its planning and operations to have flexibility in the face of unknown variables and circumstances. Unlike civilian vehicles, military vehicles are subject to harsher terrain, attacks, and at times limited logistical support. If the fuel cell system were to ever cease functioning, then having the ability to operate the vehicle on batteries only such that it can extricate itself back to a safe harbour for repairs is a desirable one. Therefore, given the minor price difference between the lowest cost configuration of $41.1931 for 8x modules in series and 1x modules in parallel, and $44.8406 for 4x modules in series and 3x modules in parallel, it may be a better option to outfit the vehicle with a slightly more expensive ESS configuration at the added benefit of increased capacity and redundancy.

Comparison to Benchmark Vehicle

Given that there is no cost comparison for the powertrain degradation pertaining to the ICEV, only the fuel component can really be looked at in terms of drawing a comparison. While hydrogen is presently more expensive than the cost of diesel fuel, the most desirable solutions for the operation profile involve using only the battery to propel the vehicle. For other operation profiles, such as ones involving longer distances, the vehicle will be required to consume more hydrogen as fuel; the tactical advantages an FCEV offers in terms of noise and thermal profile reduction must be considered a qualitative trade-off. This is in addition to the environmental considerations of ‘greening defence’ using an FCEV. In this sense, the cost extends beyond that of fuel consumption but of the lives of the soldiers themselves inside of the vehicle, which factors in as another qualitative consideration. In terms of performance, both the FCEV and ICEV were able to meet the demands for the operation profile, though the ICEV was easier to control than the FCEV in terms of applying the vehicle controller. This is not surprising, given

that the FCEV has an energy management strategy to switch between the fuel cell system, ESS and/or a combination thereof, whereas the ICEV uses the combustion engine solely as a fuel converter to provide torque to the wheels. Regarding error comparisons between the two vehicle models, the RMSE of the ICEV is an order of magnitude smaller than the mean RMSE value of the ESS configurations (0.0093 as compared to 0.0342). However, the error from both vehicle models remained low for the range of data evaluated [26], which suggests both vehicle models are adequately designed for the purposes of generating data. More specifically, [26] suggests that three times the RMSE value captures 99% of all data points; three times the mean RMSE value of all ESS configurations gives an error range up to 0.1026 km/h, which is a low value that also factors in the ESS configurations with larger error values. Regarding MAE values, the MAE for the least expensive ESS solution had a value of 0.1168, which represents the largest deviation in speed between the demanded and actual speed values. Given that a difference of 0.1168 km/h in real life is not truly discernible by a human driver, and that this maximum deviation represents 0.584% error at any given point in time, it provides additional data to suggest that the feasible solution offered by the model is acceptable. The MAE for the least expensive performs better than the ICEV value of 0.4855, and the mean ESS value of 0.4902 is almost matching that of the ICEV. In every instance of running the model, the worst waypoint across all of them never deviates more than 0.5 km/h from what is demanded, suggesting in addition to RMSE values that the model controllers are functioning adequately.

5.3. Limitations and Sources of Error for the Vehicle Model

One of the main challenges with novel research and modelling work is the paucity of existing data to use as a foundation from which to build upon. An understanding of the limitations and errors related to the results of this work is therefore imperative, such that in the future, this work may serve as a reliable baseline to build from and improve upon.

5.3.1 Model Limitations

Lack of Data Logger Information

One of the major limitations of the operation profile is the lack of data logger information, since there is no existing vehicle with which to install a data logger. A data logger would be more precise in determining vehicle speed, trip distance, and elevation instead of relying upon doctrine and software to fill in these gaps. Data loggers would also be better able to capture more realistic fluctuations in speed, including if the vehicle had to halt while on the move

during blackout conditions momentarily.

Lack of Existing Military Armoured FCEVs

Given that no military to date has fielded an FCEV military armoured vehicle, it is challenging to validate the performance of the vehicle model compared to existing FCEVs. Another limitation is that no other operation profile presently exists for the Canadian Armed Forces, making it harder to validate this work against other operation profiles. To get a better sense of validating data, this work could benefit from other work in this field to serve as a comparison. Of course, another challenge is the sensitive and secretive nature of governments providing tangible military data in a public forum. Many countries protect that kind of information and keep it in-house, leaving academia to make approximations based on available data. If the author weren't also a military officer of CAF, then the collaboration that took place generating the operation profile would likely not have occurred.

Operation Profile Design Limitations

In the absence of data logger information, equations like the Haversine equation were used to calculate vehicle distance along the operation profile pathway. The Haversine equation calculates distance along the surface of a spheroid given latitude and longitude positions, used originally in the early 19th century for naval navigation. However, the earth is not a perfect sphere but rather an oblate spheroid with an equatorial bulge, which will result in a certain amount of error during the calculation distance. However, given the relatively short distance of vehicle travel in the operation profile and the increased complexity of factoring a more accurate model of the earth into calculations, the Haversine equation was deemed adequate for calculating distance. Another operation profile limitation was the manual tracing of the operation profile pathway on Google Earth Pro for software extraction; any action performed manually has an associated operator error. The number of waypoints used in the operation profile was determined by manually selecting bends and turns along the pathway so that the defined path remained as accurate as possible. As a result, the waypoints that formed the operation profile were not equidistant, which has implications in the generation of the gradient profile. The longer the distance between waypoints, the more the elevation is linearly interpolated between point A and point B, which may smooth out any fluctuations in elevation in between the two points. However, on the other hand, too many waypoints not only increases the computational cost of the operation profile, but also increases probability of human error in generating the profile, and as well opens it to an increase in signal noise that may distract the controller and/or not best reflect the results in the model's post-processing.

5.3.2 Errors Due to Linearity

Because assumptions were needed in order to properly carry out an evaluation of the vehicle models, there are resulting errors that follow. In the case of this work, many of the assumptions made involved the use of linearity, where in reality data acquired from experimentation is non-linear in nature; however, in the absence of tangible data, without making assumptions in certain areas it would have been impossible to obtain results.

Powertrain Scaling Factors

Because the vehicle model is hypothetical and has no real world equivalent, the resulting powertrain architecture is also hypothetical. Therefore, in order to meet the vehicle's power demand for propulsion, available data from known, existing powertrain components needed to be modified in order to match the vehicle's actual speed to its desired speed. As a result, a linear scaling factor was introduced to powertrain components, where maps involving data such as torque and power outputs were scaled to be more prominent by the same scalar value. The issue with this is that not all data maps scale the same way, and in reality, may have different values when scaled to provide more significant outputs; powertrain efficiencies may also change and not be the same value when scaled. The solution to this problem would be to examine the powertrain performance of an actually fielded military FCEV, however this may still not be possible for another few years.

Powertrain Degradation Calculations

Factoring in the capital costs of the powertrain into the degradation calculations is important, as otherwise, the results would be misleading; the largest ESS configuration would then appear to be the best solution due to its shallow battery depth of discharge (DOD). However, the model assumed linear degradation per use of the operation profile, which is not how degradation works in reality. In reality, degradation is non-linear and is best represented by existing data due to fatigue analysis. While this level of fatigue analysis has been captured when evaluating the vehicle model within the confines of the singular operation profile, extracting costs associated with use over multiple operation profile trips is a linear assumption that may lead to more inaccurate results the larger the ESS configuration becomes, hence why the largest ESS configurations are amongst the most expensive options. Another factor that played into the high costs of the larger ESS configurations was the sensitivity of battery degradation in relation to the capital costs, as even small variations in value can have a significant impact on the price tag associated with the operation profile trip.

Chapter 6. Conclusion and Future Work

6.1. Summary

As part of the 'Greening Defence' initiative under the Canadian defence policy *Strong, Secure, Engaged*, the feasibility of fielding an FCEV military armoured vehicle in a tactical environment was examined. An operation profile model that emulated a path travelled by actual armoured vehicles from the Canadian Armed Forces was introduced in collaboration with the users of ICEV armoured vehicles within the Range Training Area of CFB Gagetown.

The vehicle dynamics and powertrain models of a Tactical Armoured Patrol Vehicle were introduced and implemented in MATLAB/Simulink to study the feasibility of a PEMFC-battery hybrid electric propulsion system, using the ICEV as a comparing benchmark. The performance, emissions and operating costs of the FCEV and ICEV under the newly introduced military vehicle operation profile. Different electric ESS configurations were tested in order to get a better idea of the ideal powertrain system design that best supports the operation of military vehicles at a minimum cost, consisting of the fuel consumption cost and key powertrain component performance-degradation associated costs.

This research investigated the feasibility of adopting advanced clean propulsion technology to the powertrain of armoured military vehicles. The newly introduced models and methodology support further research, design, and development of next-generation military vehicles that present a better performance in future conflict and much reduced environmental impact during routine operations and training.

6.2. Conclusions

6.2.1 Model Results

The FCEV vehicle model demonstrated that it could match the performance of the ICEV model while also having options that kept fuel costs to a minimum. Numerous areas came with sources of error when generating results. However, given the lack of available publication in this field of research, assumptions were necessary to simplify the models and make the research feasible. The RMSE and MAE values for both the FCEV and ICEV powertrain system models were within an acceptable amount of error, which meant both models were capable of matching the demanded vehicle speed. Based on minimal cost and meeting the constraint of having enough

fuel to meet the vehicle's operational range requirements, the optimal solution has 8x modules in series and 1x module in parallel.

6.2.2 Military Considerations

ESS Configuration Size

Although there is an ESS solution with a minimal cost for the operation profile, some larger ESS configurations are only slightly more expensive per operational trip. Given the nature of military operations, having built-in redundancy is worth considering when it may potentially save the lives of the soldiers inside the vehicle. In the event the fuel cell system is non-functional, having an ESS capable of bringing the vehicle back to a safe harbour for repair is worth the chain of command factoring into their decision when it comes to ESS size.

Applicability for Other In-Service Support Functions

While this work examined an operation profile under the lens of an FCEV, the concept of operation profile design has applicability now for military vehicle fleets presently operated and maintained by the Canadian Army. If existing military vehicles were converted into equivalent vehicle models, then it could be possible to better predict vehicle fuel consumption, as well as wear and tear, based on the operation or exercise undertaken. For example, every year, the Canadian Army holds Exercise MAPLE RESOLVE as a means of evaluating unit readiness to deploy somewhere in the world if called upon [27]. Part of this exercise involves training with vehicles that take predetermined routes based on the exercise scenario. The Canadian Army relies upon historic data from previous years to order parts to provide maintenance and logistical support for the exercise, but if the scenarios were able to be translated into a series of operation profiles, a more accurate prediction of fuel consumption and spare parts can be made, thus potentially saving the government on taxpayer dollars during major exercises such as MAPLE RESOLVE. The same principle applies to considering deploying to a theatre of operations around the world. An operation profile can be created and evaluated based on likely scenarios, thus enabling the chain of command to get a rough idea of costing before ever having to physically touch the ground. The Canadian Armed Forces have geo-techs whose function is to provide terrain analysis to commanders who make decisions. Therefore this type of analysis is feasible within the current framework of the Canadian Armed Forces today.

6.3. Research Contributions

The original research contributions of this work can be summarized as:

- An operational profile was introduced for a military armoured vehicle model. To ensure the general applicability, this profile was built without using data loggers or other operation data collection devices on a specific vehicle, instead the generic operation profile was introduced using stakeholder input and military doctrine.
- Using the existing vehicle structure from the most comparable vehicle model available, a military armoured vehicle model was developed, which is an approximation of the TAPV currently fielded by the Canadian Army. This FCEV was also designed to meet specific operational requirements while having zero pump-to-wheel emissions, which is a functional improvement over existing Canadian military vehicle fleets.
- Performance degradation models of both PEMFC and $LiFePO_4$ battery were implemented to support the prediction of operational costs associated with the more realistic performance degradations of PEMFCs and battery ESS.
- With the information available, a comparison was drawn between an FCEV and ICEV military vehicle models, pertaining to cost of fuel consumption and overall vehicle model error between actual and demanded vehicle speeds. The comparison is made to show the cost and emission differences of the new FCEVs.
- This research conducted a feasibility study on a military armoured FCEV operating in blackout conditions on a convoy move, and has opened new paths for further studies of other tactical and operational scenarios to include examples such as future studies in arctic and desert environments.

6.4. Future work

Given that this work is among the first to be published in the field of military armoured FCEVs, much can be done to build upon and improve the results from this work. Three major areas that can be improved upon are: increased number of operation profiles, more accurate powertrain data, and considering the use of a HESS powertrain configuration for the vehicle model.

6.4.1 Additional Operation profiles

Given that the CAF deploys to locations all around the world, there are many more operation profiles that can be developed. Mountain warfare, jungle warfare, desert warfare, arctic warfare, and urban warfare are all within the spectrum of conflict undertaken by the CAF, and each one can have a series of operation profiles associated with it. Convoy moves and simulated attacks are two of many options that can be modelled and costed for creating a repository of information that the chain of command can refer to not only for current operations, but also when writing the Statement of Requirement (SOR) for the acquisition of future fleets via crown project contracts.

6.4.2 More Accurate Powertrain Data

Once actual military armoured FCEVs get fielded and used by governments, data loggers can be used to acquire more accurate powertrain data, which in turn enables the design of a more accurate vehicle model. This would help to address issues with assumptions related to linearity in this work, and would lead to more accurate cost estimates, which in turn would lead to more accurate budget forecasting, and ultimately better allocation of taxpayer dollars.

6.4.3 Integration of an HESS into the Vehicle Model

Although it was attempted during this work, the integration of a battery and ultracapacitor combination into the FCEV powertrain was unsuccessful due to its complexity. A HESS configuration is a desirable option to evaluate: given the ultracapacitor's ability to be activated during peak power demands, it would reduce the peak power demand on the battery, and thus reduce battery degradation losses. Ultracapacitors also have the added benefit of superior performance in hot and cold environments as compared to a lithium-ion battery, making them an appealing option for operations in both desert and arctic environments. It is suspected that an HESS configuration would therefore result in less expensive vehicle use, and as such should be pursued in future work.

References

[1] “The Paris Agreement”. United Nations Framework Convention on Climate Change. Le Bourget, France, 4 November, 2016. https://unfccc.int/process-and-meetings/the-paris-agreement/the-paris-agreement.

[2] “Strong, Secure, Engaged”. Canada Defence Policy. pp 76 (102), Canada, 2017. https://www.canada.ca/en/department-national-defence/corporate/policies-standards/canada-defence-policy.html.

[3] Manoharan, Y.; Hosseini, S.E.; Butler, B.; Alzhahrani, H.; Fou Senior, B.T.; Ashuri, T. “Hydrogen Fuel Cell Vehicles; Current Status and Future Prospect”. OrcID and John Krohn Combustion and Sustainable Energy Laboratory (ComSEL), Department of Mechanical Engineering, Arkansas Tech University, 1811 N Boulder Ave, Russellville, AR 72801, USA.

[4] J4 Move Doc. “Joint Doctrine Manual: Road Movement”. B-GJ-005-404/FP-030. Canada. 12 June, 2003.

[5] Lopez, J. “GM Hydrogen Fuel Cell Vehicle On The Horizon For The Military”. GM Authority Blog, October 29, 2020. https://gmauthority.com/blog/2020/10/ gm-hydrogen-fuel-cell-vehicle-on-the-horizon-for-the-military/.

[6] Edsall, L. “Kia unveils military grade all-terrain vehicles”. Classic Cars Journals, November 4, 2020. https://journal.classiccars.com/2020/11/04/kia-unveils-military-grade-all-terrain-vehicles/.

[7] “Vehicle and Fuel Emissions Testing: Dynamometer Drive Schedules.” US Environmental Protection Agency (EPA). March 19, 2021, https://www.epa.gov/vehicle-and-fuel-emissions-testing/dynamometer-drive-schedules.

[8] Feng, Y.; Dong, Z. “Optimal energy management strategy of fuel-cell battery hybrid electric mining truck to achieve minimum lifecycle operation costs”. *Int J Energy Res*. 2020; 44: 10797– 10808. https://doi.org/10.1002/er.5728

[9] Han, D.S.; Choi, N.W.; Cho, S.L.; Yang, J.S.; Kim, K.S.; Yoo, W.S.; Jeon, C.H. “Characterization of driving patterns and development of a driving cycle in a military area”. *Transportation Research Part D: Transport and Environment*, 2012; 17(7): 519-524. https://doi.org/10.1016/j.trd.2012.06.004

[10] “Coefficients of Friction of Various Roadway Surfaces”. Texas Claims & Consulting Company. Publishing date unknown. https://marules.com/wp-content/uploads/Adj-FrictionCoefficients-VariousRoadwaySurfaces.pdf.

[11] Director of Army Doctrine. “Land Operations”. B-GL-300-001/FP-001. 1 January, 2008.

[12] Liu, J.; Dong, H.; Jin, T.; Manouchehrinia, C.; Dong, Z. “Optimization of Hybrid Energy Storage Systems for Vehicles with Dynamic On-Off Power Loads Using a Nested Formulation”. *Energies,* 2018; 11(10): 2699.https://doi.org/10.3390/en11102699.

[13] Baronas, J.; Achtelik, G. “Agency Staff Report on Assembly Bill 8: 2019 Annual Assessment of Time and Cost Needed to Attain 100 Hydrogen Refueling Stations in California”. California Energy Commission. Technical report number CEC-600-2019-039. December 30, 2019. https://ww2.energy.ca.gov/2019publications/CEC-600-2019-039/CEC-600-2019-039.pdf

[14] “Elevation Profile Extraction Software,” https://gpsvisualizer.com.

[15] “Haversine Formula,” https://en.wikipedia.org/wiki/Haversine_formula#cite_note-Gade2010-9.

[16] Feng, Y. “Documents for Commercial Truck Models”. University of Victoria, Victoria, BC, Canada, 2020. (Unpublished)

[17] “Tactical Armoured Patrol Vehicle,” https://en.wikipedia.org/wiki/Textron_Tactical_Armoured_Patrol_Vehicle.

[18] Thatcher, C. “Defining the TAPV”. Canadian Army Today. December 5, 2017. https://canadianarmytoday.com/defining-the-tapv/.

[19] “16.00R20 Michelin XZL Tire”. Military Tires Website. Technical Specifications. 2021. https://militarytires.ca/product/16-00r20-michelin-xzl/.

[20] Chen, L.; Tong, Y.; Dong, Z. “Li-Ion Battery Performance Degradation Modeling for the Optimal Design and Energy Management of Electrified Propulsion Systems”. *Energies*, 2020; 13(7): 1629. https://doi.org/10.3390/en13071629.

[21] Amzallag, C.; Gerey, J.P.; Robert, J.L.; Bahuaudl, J. “Standardization of the rainflow counting method for fatigue analysis”. *International Journal of Fatigue,* 1993; 16: 287-293. https://doi.org/10.1016/0142-1123(94)90343-3.

[22] Muenzel, V.; de Hoog, J.; Brazil, M.; Vishwanath, A.; Kalyanaraman, S. “A Multi-Factor Battery Cycle Life Prediction Methodology for Optimal Battery Management”. *Proceedings of the 2015 ACM Sixth International Conference on Future Energy Systems* (e-Energy '15). Association for Computing Machinery, New York, NY, USA, 2015: 57–66. https://doi.org/10.1145/2768510.2768532.

[23] Shi, Y.; Xu, B.; Tan, Y.; Zhang, B.“A Convex Cycle-based Degradation Model for Battery Energy Storage Planning and Operation”. *2018 Annual American Control Conference (ACC)*, 2018, pp. 4590-4596. https://doi.org/10.23919/ACC.2018.8431814.

[24] “Mathworks - Rainflow Function," https://www.mathworks.com/help/signal/ref/rainflow.html

[25] “Energy Sources - Average Retail Prices for Diesel in Canada". Natural Resources Canada, Ottawa, Canada, 2019. https://www2.nrcan.gc.ca/eneene/sources/pripri/prices_byyear_e.cfm?ProductID=5

[26] Spiegel, M.R.; Schiller, J.; Srinivasan, R.A.“Standard Error of Estimate". Probability and Statistics, 4th Edition, Mc-Graw Hill Companies Inc., 2013.

[27] “Exercise MAPLE RESOLVE". Canadian Armed Forces, Government of Canada, Ottawa, Canada, 2021. http://www.army-armee.forces.gc.ca/en/exercises-operations/ex-maple-resolve.page

Appendix A- Operation Profile Planning Map

The image in Annex A depicts the RTA of CFB Gagetown, and the real pathway taken by the vehicle model to represent a convoy move. The start point for the pathway starts in the top left grid square 975 783 (denoted by the dashed green pathway), where the vehicle leaves the base and drives east toward the RTA, where it then proceeds to complete a loop that serves as the distance and elevation basis of the operational profile. The type of map generated was in collaboration with 4 ESR, and is the type of map used in regular military planning and operations.